Human and climate-environment interactions in Pyrenean landscapes: a Lateglacial-Holocene multiproxy reconstruction

Irene Julián-Posada[1, 2], Graciela Gil-Romera[1], Ana Moreno[1], Bérangère Leys[3], Blas Valero-Garcés[1], Penélope González-Sampériz[1]

[1]Instituto Pirenaico de Ecología (IPE-CSIC), Zaragoza, 50059, Spain
[2]Escuela de Doctorado de la Universidad Autónoma de Madrid (EDUAM), Madrid, 28049, Spain.
[3]IMBE, Aix Marseille Université, Avignon Université, CNRS, IRD, Aix-en-Provence, 13545, France

Correspondence to: Irene Julián-Posada (irenejulianp@gmail.com)

Abstract. Mountain ecosystems present a complex challenge in disentangling the drivers of their long-term transformation. The subalpine belt of the Pyrenees, once forested, is now characterised by a mosaic of forest patches and open landscapes, and has represented a key region in herding practices until last century, when land-use changes have led to a reforestation of this area. However, the relative contributions of climate and human activity in driving its change remain intensely contested. We present a high-resolution, multi-proxy reconstruction of landscape dynamics over the last 25,000 years from the southern Pyrenees. We have integrated mammal herbivores, fire regime and vegetation dynamics through sedimentary ancient DNA, pollen and charcoal analyses. With this approach, we aim to compare these proxies and identify the timing and drivers of vegetation change and to distinguish anthropogenic from climatic forces. Our results reveal a multi-phase evolution, with Lateglacial and postglacial forest expansion followed by Mid-Holocene openness, initially triggered by the cooling at the initial phase of the Neoglacial period, but subsequently maintained by pastoral activities. We find that humans opportunistically exploited this openness from the Mid-Holocene onwards, later transitioning to active landscape management through fires and grazing. This study demonstrates that current Pyrenean landscapes are not a product of exclusively humans or climate, but of their synergy over millennia. Effective conservation strategies must integrate an understanding of this deep ecological history with the emulation of traditional practices to preserve these unique, human-shaped biodiversity hotspots.

1 Introduction

Global Change has profoundly and irrevocably impacted ecosystems worldwide (Aurelle et al., 2022), with mountains experiencing disproportionate transformations due to their sensitivity to climatic shifts and human pressures (Steinbauer et al., 2018). In these regions, complex topography fosters ecosystem mosaics where subtle changes in temperature, water availability, or land use can trigger cascading ecological effects (Hock et al., 2019; Padilla et al., 2010; Viviroli et al., 2011). Understanding these dynamics requires disentangling natural variability from anthropogenic forces, a challenge especially salient in regions like the Mediterranean Basin, where human-environment interactions span millennia. The Iberian Peninsula exemplifies this complexity: its convergence of climatic, geological, biogeographical, and historical conditions has generated exceptional environmental heterogeneity, resulting in a patchy and highly diverse vegetation landscape since the Pleistocene, where open ecosystems predominated over dense forests (Carrión et al., 2010; González-Sampériz et al., 2010).

While tracing past human activities has been the subject of several global initiatives (e.g. the *Human traces* initiative in PAGES: https://pastglobalchanges.org/human-traces), distinguishing anthropogenic from natural drivers in sedimentary records remains contentious (Felde et al., 2024). This is especially challenging in the Mediterranean region, where traditional anthropogenic indicators such as key pollen taxa (e.g. *Olea*, *Plantago*) and/or sudden declines in arboreal pollen percentages can reflect both human activity and climatic variability (Deza-Araujo et al., 2020). The Pyrenees, a region with a long-standing history of human presence (Gassiot-Ballbè et al., 2017; Utrilla et al., 2012), and particularly sensitive to both past and recent environmental changes (González-Sampériz et al., 2017), epitomize this challenge. This mountain range served as a corridor for Neolithic expansion (Gassiot-Ballbè et al., 2017; Julián-Posada et al., 2025) and a natural laboratory for agro-pastoral

adaptation. From Neolithic agro-pastoralism to Medieval fire use, we know that human activities have fundamentally influenced and shaped terrestrial ecosystems for a long time (García-Ruiz et al., 2015; Montes et al., 2020). Among these, herding has been hypothesised as a key driver maintaining open landscapes (García-Ruiz et al., 2020b), but its timing, ecological impact, and interplay with climate remain unresolved.

The subalpine belt in the Pyrenees, like in other European mountains (Dietre et al., 2020; Dziomber et al., 2024; Fabre et al., 2023; Vincze et al., 2017; Wick et al., 2003), was forested at the Holocene onset, and gradually transformed into today's open landscapes. In the Pyrenees, this transformation began during the Bronze Age (4 ka BP), though became evident since the Middle Ages (González-Sampériz et al., 2017, 2019). Pastoralists have dynamically used this subalpine belt, taking advantage of its productive pasturelands for grazing through the practice of transterminance (García-Ruiz et al., 2020b; Oteros-Rozas et al., 2013). This practice involves the seasonal movement of livestock between lowland and upland areas within the same mountain system, and has been actively maintained by herding communities since Neolithic times (Casas and Gassiot-Ballbè, 2022).

Determining whether Pyrenean landscapes are maintained by human action (e.g. pastoralism, fire) has profound implications (García-Ruiz and Lasanta, 2018). If pastoralism actively sustained open ecosystems over millennia, these landscapes represent a cultural heritage with unique biodiversity shaped by human stewardship (Ellis, 2021; Oteros-Rozas et al., 2013; Plieninger et al., 2015). Conversely, if openness primarily reflects climatic drivers, their resilience to modern land-use abandonment may differ (Navarro and Pereira, 2015). Resolving this dichotomy is critical for conservation: cultural landscapes require management strategies that emulate traditional practices, while naturally open systems may need climate-centric protections. Pastoralism's role, whether as a primary architect or secondary modifier of ecosystems, also informs debates about rewilding, carbon storage, and the preservation of montane biodiversity hotspots (Dietre et al., 2020; García-Ruiz et al., 2020b). While some studies suggest that human impact exists since the Early Holocene through pastoralism or deforestation practices with fire (Ellis, 2021; Galop, 2016; Gassiot-Ballbè et al., 2017; Vannière et al., 2016), others point to the Middle Ages as the moment when this impact became evident at a regional scale (González-Sampériz et al., 2017). This persistent lack of consensus underscores the need for new high-resolution, multi-proxy studies to definitely disentangle these intertwined influences.

Here, we aim to improve our understanding of landscape dynamics in the Pyrenees, by reconstructing the history of Tramacastilla Lake sequence (1682 m a.s.l.). First, we want to compare methodological approaches of past vegetation reconstruction, based on fossil pollen and *sed*aDNA analyses. Second, we aim to identify the timing and underlying drivers of subalpine landscape transformation through the comparative analysis of regional and local vegetation records, and situate the findings within the broader palaeoenvironmental context of the Pyrenees and Southern Europe. In order to pursue our objectives, we present a centennial to millennial time scale environmental multiproxy reconstruction for the last 15,000 years at Tramacastilla lake, that includes the previously published first *sed*aDNA continuous record of human-environment interactions over the Holocene in the Iberian Peninsula (Julián-Posada et al., 2025). Through an integrative approach, our study establishes a framework for assessing unequivocal anthropogenic footprints in sensitive mountain ecosystems.

2 Material and Methods

Geographical setting

Tramacastilla Lake (TRAM) (42°43'31.57"N, 0°22'03.73"W) is located at 1682 m a.s.l. in the Upper Gállego Valley, southern Pyrenees (Huesca, NE Spain) (**Fig. 1**). It was formed in a deepened hollow between two glacial valleys, which were tributaries to the primary glacier in the Gállego Valley (Garcia-Ruiz and Valero-Garces, 1998). The lake basin is about 50 ha, fed by small creeks, and consists of Devonian sandstones and shales (García-Ruiz et al., 2001). Tramacastilla Lake was dammed in 1956, having a previous maximum depth of 4.5 m, while it currently reaches 13 m. It is situated in the subalpine belt, and the surroundings of the lake consist of an open landscape dominated by grasslands, and scattered trees and shrubs (*Pinus uncinata* Ramond ex DC., *Pinus sylvestris* L., *Rosa* sp., and *Juniperus communis* L.). The vegetation of the Upper Gállego Valley (**Fig. 1b**) is equally dominated by open landscapes, where pastures prevail in the areas close to the Gállego river, and subalpine and alpine meadows occupy the highest altitudes, as well as human-deforested areas. Mixed deciduous forests (i.e. *Betula* sp., *Corylus* sp., *Acer* sp., *Fraxinus* sp.) appear in mid altitudes (1500-1600 m a.s.l.), while conifers occupy high areas between 1600 m and the timberline ecotone (upper limit of dense forests), which is situated at 1700-1800 m, although some isolated trees can be found up to the treeline (limit of arborescent growth forms), at 2000-2200 m (Villar and Sesé, 1999). In the transition of the montane and subalpine belts, *Abies* and *Fagus* forests are found. Located in one of the western valleys of the Central Pyrenees, the climate in Tramacastilla has influences from both Mediterranean and Atlantic regimes, with a current mean annual precipitation of about 1400 mm. The average annual temperature is 7ºC, with an average minimum temperature in summer of 13ºC and a maximum of 25ºC, whilst in winter the average minimum is -3ºC and the average maximum is 5ºC (**Fig. 1 c, d**).

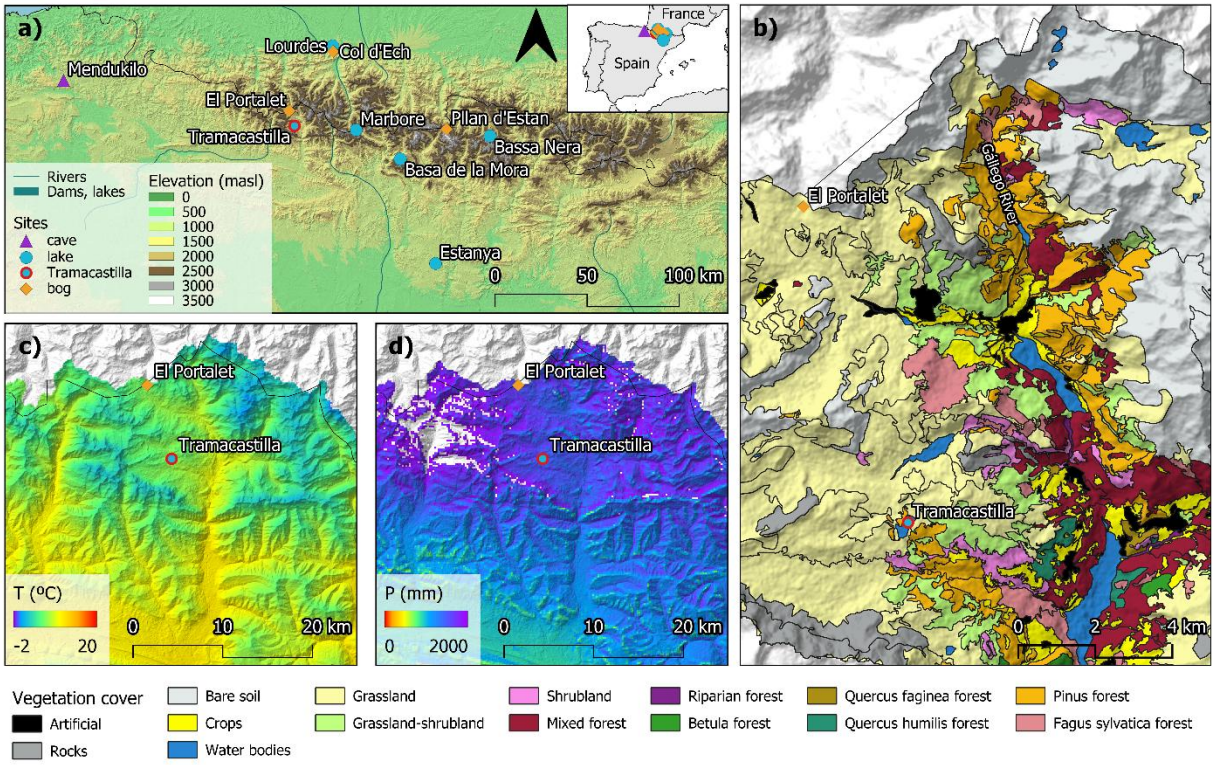


Figure 1: Location map of Tramacastilla lake and other records cited in this article. Includes: a) altitude map; b) regional vegetation map; c) mean annual temperature; and d) mean annual precipitation. ASTER GDEM data courtesy of METI and NASA. Spanish Forest Map © MITECO (1:25000), © IGN-CNIG (1:200k). Digital Climatic Atlas of the Iberian Peninsula © Ninyerola et al. (2005). Projection UTM30 Datum ETRS89 (EPSG: 25830). All coordinates in **Supplementary Data 8**.

2.2 Core sampling, facies description and age-depth model

We retrieved two sediment cores using a UWITEC platform in October 2020 (TRAM20-1A and TRAM20-1B), and two in October 2021 (TRAM21-1A and TRAM21-1B) in the deepest part of Tramacastilla Lake (13.5 m). Each core was about 9 m long, and divided in 5 sections (1U-5U) according to the extraction operations using the UWITEC platform. All cores were opened, longitudinally cut and described in terms of basic sedimentological aspect. We selected TRAM20-1B and TRAM21-1B for analyses, they were then photographed, stored at 4ºC at the Pyrenean Institute of Ecology (IPE-CSIC, Zaragoza) and sampled for biotic and abiotic analyses. They were sedimentologically correlated, based on the lithofacies and AMS radiocarbon dates of both cores (**Fig. A1**). Lithofacies were defined based on macroscopic characteristics including colour, mineral composition and grain-size sedimentary structures assessed through microscopic smear slide observations, following the method proposed by Schnurrenberger et al. (2003) (**Table B1**).

Uppermost sections (1U and 2U) from selected cores displayed sediments that are a product of high-energy depositional processes without in-lake organic production, that may include reworked organic material into the sediment, resulting in a non-coherent chronology. Given this condition, these sections have been excluded from the age-depth model and biological

analyses. This decision is also supported by X-Ray Fluorescence data (**Fig. 2**), that shows differences in the composition between the first two sections and the others (low organic carbon and low Fe/Mn ratio). Then, the final age control of the composite lacustrine sequence of Tramacastilla is based on 21 calibrated AMS radiocarbon dates from bulk sediment samples from core TRAM20-1B, and 1 from core TRAM21-1B (**Table 1**, **Fig. A1**), as no terrestrial plant macrofossils were found in the sediment. These dates were performed at DirectAMS Radiocarbon Dating Service (Seattle, USA). We produced a Bayesian age-depth model for the sediment between 390 cm and 880 cm depth, using 'rbacon' package v. 3.3.1 (Blaauw and Christen, 2011) and IntCal20 calibration curve (Reimer et al., 2020) (**Fig. 3**). All procedures for building the chronology are detailed in **Appendix A1**.

Table 1: Calibrated AMS radiocarbon dates used for building the chronological model of the sequence.

labID	Age (yr BP)	Error	Depth (cm)	Mean calibrated age, 2σ (IntCal20) ± standard deviation (cal yr BP)	Dated material	95% Confidence Interval	Age in the figures (median, cal yr BP)
TRAM20-1B-3U 19-20	920	25	390.9	838 ± 49	Bulk	772 - 937	863
TRAM20-1B-3U 42-44	1685	20	429.5	1585 ± 52	Bulk	1540 - 1744	1611
TRAM20-1B-3U 56-58	2125	25	452	2104 ± 76	Bulk	2054 - 2385	2192
TRAM20-1B-3U 75-76	3035	25	480.9	3240 ± 67	Bulk	3138 - 3360	3255
TRAM20-1B-3U 88-89	3435	25	501.8	3698 ± 67	Bulk	3589 - 3828	3689
TRAM20-1B-3U 112-113	3810	25	540.4	4201 ± 67	Bulk	4129 - 4421	4250
TRAM20-1B-4U 26-27	4745	35	571.4	5480 ± 79	Bulk	5353 - 5597	5509
TRAM20-1B-4U 41-42	5110	25	596	5833 ± 61	Bulk	5766 - 5969	5840
TRAM21-1B-4U 21-22	5360	25	620	6143 ± 82	Bulk	6079 - 6366	6260
TRAM20-1B-4U 70-71	6410	25	643.4	7340 ± 55	Bulk	7260 - 7573	7415
TRAM20-1B-4U 97-98	8400	30	687.6	9416 ± 68	Bulk	9314 - 9592	9484
TRAM20-1B-4U 115-116	9830	40	717.1	11254 ± 92	Bulk	10955 - 11455	11280
TRAM20-1B-5U-1 27-28	10160	35	750.5	11786 ± 131	Bulk	11707 - 12441	11905
TRAM20-1B-5U-1 41-42	10805	40	765.2	12760 ± 41	Bulk	12774 - 13126	12921
TRAM20-1B-5U-1 57.5-59	12440	50	783.1	14603 ± 200	Bulk	13906 - 14578	14277
TRAM20-1B-5U-1 69-71	12260	60	795.8	14294 ± 228	Bulk	14150 - 14786	14430
TRAM20-1B-5U-2 10.5-12	12395	45	815.8	14534 ± 205	Bulk	14477 - 15095	14822
TRAM20-1B-5U-2 24-25.5	12885	40	829.4	15409 ± 105	Bulk	15214 - 15738	15471
TRAM20-1B-5U-2 33-35	16565	50	840	20012 ± 128	Bulk	20280 - 20905	20639
TRAM20-1B-5U-2 45-46.5	18645	70	851.6	22588 ± 149	Bulk	22460 - 23010	22675
TRAM20-1B-5U-2 58.5-60	19925	80	866.3	23965 ± 143	Bulk	23767 - 24403	24062
TRAM20-1B-5U-2 72-74	20920	80	881	25221 ± 194	Bulk	24219 - 25350	25014

2.3 Geochemical, magnetic and elemental composition analyses

Core TRAM20-1B was selected for these analyses due to its excellent continuity. Magnetic Susceptibility (MS) was measured every 1-cm using a high-resolution point sensor (MS2E) mounted in a GEOTEK Multi-sensor Core Logger at the Pyrenean Institute of Ecology (IPE-CSIC, Spain) laboratories. Elemental composition analyses were performed to estimate total organic (TOC) and inorganic (TIC) carbon, total Sulphur (TS) and total Nitrogen (TN) content at 2-cm resolution by infrared absorption of CO_2 liberated by combustion in a LECO CNS 928 analyser at the Scientific and Technique Soil Analysis Service of IPE-CSIC. Elemental geochemical composition was analysed using an AVAATECH X-Ray Fluorescence (XRF) Core Scanner at 10 kV and 30 kV (15s and 45s time span respectively), at 5 mm intervals at the CORELAB laboratory at the Universitat de Barcelona (Spain). Some elements (Ti, K, Si, S and Br) and ratios (Ca/Ti, Fe/Mn, Rb/Zr) were selected from XRF analysis because of their significant value in the sediment composition, as indicators of siliciclastic supply (Ti, K, Si) carbonate productivity (Ca/Ti), sediment fluxes (Rb/Zr), organic content (S, Br) and redox conditions (Fe/Mn).

2.4 Pollen analysis

Pollen extractions were made at the Laboratory of Palaeobiological Indicators in IPE-CSIC, following the standard chemical procedure (Moore et al., 1991), including Thoulet solution for separation (density = 2 g/cm^3) and the addition of two tablets of *Lycopodium clavatum* spores to each sample (20848 spores per tablet), in order to estimate concentrations (Stockmarr, 1971). Samples were mounted in glycerine, and pollen grains were identified using an optical microscope (Leica DM750), with help of the reference pollen collection of IPE-CSIC and identification keys and photographic atlas (Moore et al., 1991; Reille, 1992). A total of 111 samples were analysed at 2–3 cm resolution for the entire core TRAM20-1B (starting at 380 cm depth), except for section 5U, which was sampled at 5 cm intervals. Pollen counts were conducted until a minimum of 300 terrestrial grains was reached, ensuring sufficient representation as indicated by the plateauing taxa accumulation curve (no additional pollen types were identified beyond this threshold). This approach is grounded in the use of taxa accumulation curves as a robust method for assessing palynological richness (Giesecke et al., 2014).

We calculated Pollen Accumulation Rates (PAR or influx: number of pollen grains·cm^{-2}·yr^{-1}), as a proxy for plant abundance. PAR is a metric more closely related to plant biomass and less conditioned by variable sedimentation rates and biased by counts. Since pollen output is generally proportional to plant abundance and productivity, PARs offer a reliable estimate of above-ground biomass, particularly when calibrated with sedimentation rates (Knight et al., 2022; Matthias and Giesecke, 2014; Seppä et al., 2009). Consequently, PAR and biomass will be used interchangeably in the current study.

To facilitate data visualisation and interpretation, we classified pollen types and spores into 37 different groups, considering both individual taxa and functional properties (**Supp. Data 1**). For discussing results, we added an "Anthropogenic taxa" group, that includes those taxa that have traditionally been associated with human activities (Connor et al., 2019; Deza-Araujo et al., 2022): Cerealia type, *Plantago*, *Plantago* t. *media/major*, *Rumex* and *Urtica*. We also added a category for "Steppe taxa", including *Ephedra*, *Artemisia*, Asteraceae (*Centaurea*, Cichorioideae, Asteroideae, *Carduae*), Brassicaceae, Caryophyllaceae,

Caryophyllaceae t. *Spergularia*, Chenopodiaceae and Cistaceae t. *Helianthemum* (**Supp. Data 1**). Cluster analyses, based in Constrained Incremental Sum of Squares (CONISS) algorithm (Grimm, 1987), were used to define pollen zones, and were performed with vegan R package v. 2.6-10 (Oksanen et al., 2022). Pollen diagrams were plotted using rioja R package v. 1.0-7 (Juggins, 2024), and discussion figures with ggplot2 R package v. 3.5.1 (Wickham et al., 2025).

2.5 Charcoal analysis

We analysed 202 contiguous samples from sections 3U and 4U of the Tramacastilla lacustrine sequence (TRAM20-1B) at a 1-cm resolution, focusing on the Holocene to capture centennial-scale environmental variability. This interval was selected to ensure precise chronological alignment with known climatic transitions and regional palaeoenvironmental records. Charcoal particles from sediment samples were extracted at the Scientific and Technique Sedimentary Analysis Service of IPE-CSIC following the chemical protocol from Daniau et al. (2007). This procedure implied a sample digestion with 30% H_2O_2 added to 1.5 g of wet sediment over 24h. The bleached sample was then filtered using a 62-µm sieve and the fraction recovered with distilled water.

Charcoal particles were counted using *Win seedle* Pro 2020a software (Regent Instrument Inc., 2023) with a ZEISS stemi 508 063 microscope. This software takes measurements of the total area (μm^2), and the width-to-length (W/L) ratio of each charcoal particle. The W/L ratio serves as an indicator of the type of fuel consumed during burning, with values below 0.5 suggesting that at least 40% of the burnt vegetation consists of grasslands, and values above 0.5 indicating a predominance of woody vegetation being burnt (Daniau et al., 2007; Leys et al., 2017). Particles with an area smaller than 12100 µm² (equivalent to a 110-µm sieve) were excluded from further analysis in order to minimise noise and enhance the representation of local vegetation (Leys et al., 2017). We represent charcoal data as Charcoal Accumulation Rate (CHAR: $\mu m^2 \cdot cm^{-2} \cdot yr^{-1}$), as it quantifies the influx of charcoal particles into sediments over time. Unlike simple charcoal concentration (e.g., particles per cm^3 of sediment), CHAR integrates the effects of variable sediment accumulation rates, providing a more accurate measure of fire activity over time. To estimate CHAR, the total area of all particles within a sample was considered instead of the total number of charcoal particles in order to avoid particle fragmentation biases (Ali et al., 2009; Tinner and Hu, 2003) (both parameters are correlated: Spearman test with p-value < 0.05 and Rho = 0.86; and this correlation is linear: $R^2 = 0.78$).

To reconstruct regional and local fire activity, we used the long-term trend of CHAR based on time-series analyses from Higuera et al. (2010). Numerical analyses of charcoal data were performed using 'tapas' R package v.0.1.3 (Finsinger and Iago-Lito, 2022), and following Finsinger et al. (2014). This approach decomposes charcoal accumulation data into two components: a background trend, representing regional or long-term charcoal input, and peaks, which are interpreted as evidence of local fire episodes. Charcoal data was interpolated to a constant temporal resolution of 35 years and then broken down into a low-frequency background component and a peak component, using a robust locally weighted polynomial regression with a moving-window width of 600 years. This results in a robust Signal-to-Noise Index (SNI) (Kelly et al., 2011). The peaks were evaluated using the 95^{th} percentile of the modelled noise distribution obtained, therefore considered fire

occurrences, to eventually calculate the fire return intervals (FRI: years between two consecutive fire episodes) (Higuera et al., 2010).

2.6 *sed*aDNA analysis

Sedimentary Ancient DNA (*sed*aDNA) was previously analysed for 46 samples of core TRAM21-1B for plants and animals through a metabarcoding approach. Procedure and results for this analysis are described in Julián-Posada et al. (2025). For a better discussion comparing with pollen data, we incorporate two groups: "Anthropogenic taxa", that includes those sequences clearly identified as taxa associated with human activities following Connor et al. (2019) and Deza-Araujo et al. (2022) (e.g. Brassicaceae, *Urtica dioica*, *Hordeum*, *Plantago*, *Rumex*); and "Steppe taxa", that comprises Asteraceae, Chenopodiaceae, Brassicaceae, *Helianthemum*, *Artemisia*, *Plantago*, *Rumex*, and *Ephedra*.

3 Results

3.1 Sedimentology and geochemistry

The Tramacastilla Lake sequence presents 9 sedimentary facies (**Fig. 2**) and has been divided into 5 sedimentary Units, mainly formed by siliciclastic silts and clays. All sedimentary facies are described in **Table B1**, and all sedimentological and geochemical measurements are shown in **Fig. B1**.

Sedimentary Units 1 and 2 present mm-thick banded silts and clays (**Fig. A1**). Based on geochemical and mineralogical measurements (**Fig. 2**), these units are made by a constant and high external input of sediment into the lake, indicated by stable values of MS and changes in Ti, K and Si values. The most oxidised conditions are recorded, denoting a low lake level and low organic content, suggested by reduced values in the Fe/Mn ratio. The generally low TIC values and Ca/Ti ratio reflect the lack of carbonates, except for some thin red laminae in Unit 1 and 2 (**Table B1**). Low values of TOC, Br and TOC/TN support reduced organic content in the sediment, and therefore a low lake productivity during this period. Finally, Unit 1 is characterised by a higher proportion of silt compared to Unit 2, as evidenced by variations in the Rb/Zr ratio.

Sedimentary Units 3 and 4 exhibit massive to banded sediments (**Fig. 2** and **Fig. B2**) and reduced external input, as indicated by lower MS, Ti, K, and Si values compared to Units 1 and 2. Increasing Fe/Mn ratios point to more anoxic conditions in a deep organic-rich lake. TOC begins to rise, marking the most organic-rich phase, supported by high Br values that reflect peak lake productivity. This phase coincides with diminished external input, and TOC/TN ratios suggest a dominance of terrestrial over aquatic vegetation. Sediment grain size remains small, similar to Unit 1, as shown by Rb/Zr values.

Unit 5 displays a pattern similar to Units 1 and 2, with renewed external sediment input reflected by elevated Ti, K and Si values. TOC/TN, TOC, and Br values decline relative to Units 3 and 4, indicating reduced organic content. A drop in the Fe/Mn ratio suggests a return to lower lake levels. The Rb/Zr ratio also decreases, denoting coarser grain size, consistent with sedimentary facies descriptions (**Table B1**).

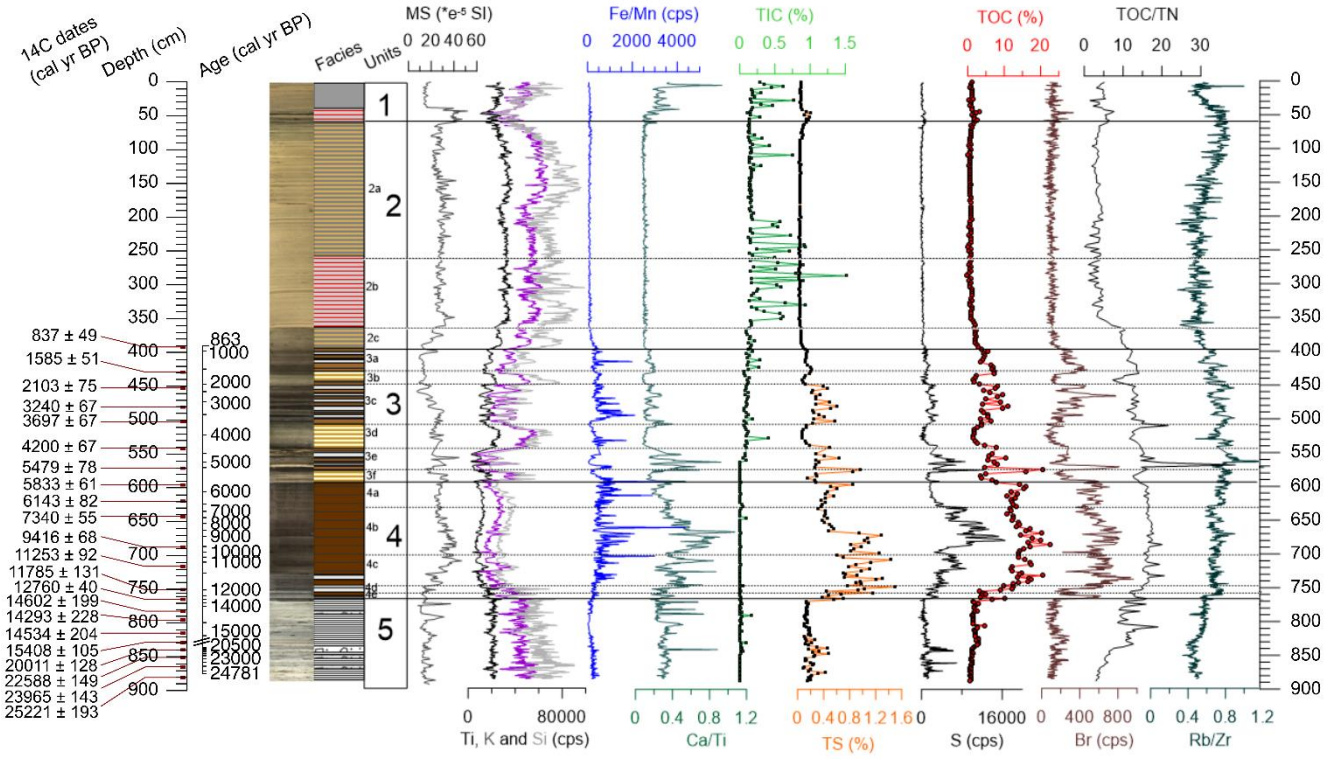


Figure 2: Synthesis of mineralogical and geochemical results for Tramacastilla sequence. Includes: AMS calibrated dates, depth, age, high-resolution photo, sedimentary facies with units and subunits; MS - magnetic susceptibility (SI x 10-5); selection of X-Ray fluorescence data (Ti, K, Si, Fe/Mn, Ca/Ti, S, Br, Rb/Zr, measured in counts per second); TIC - total inorganic Carbon (%); TS - total Sulphur (%); TOC - total organic Carbon (%) and TOC/TN.

3.2 Age-depth model

Between 25 and 22 ka BP we found a sedimentation rate of 0.01 ± 0.03 cm/yrs (**Fig. A2** and **Fig. 3**), pointing again to a high-energy depositional environment in a vegetation-barren landscape and soil. From 22 to 20 ka BP, the sedimentation rate is very low, probably indicating the lake was frozen most of the year under very cold conditions, that perhaps limited local primary production. Between 20 and 15 ka BP, the record reflects a sedimentary hiatus. A more stable sedimentation rate is recorded between 15 and 0.8 ka BP (0.045 ± 0.02 cm/yrs), with some parts of high values at ca. 15 ka BP, at the beginning of the Holocene, at around 6 ka BP and from 4 ka BP onwards (**Fig. A2**). Thus, we present the entire record spanning 880 to 380 cm (25–0.8 ka BP), but focus our discussion on the interval between 820 and 380 cm, once the organic lacustrine sedimentation started. This section includes the Lateglacial period—Bølling (14.7–14 ka BP), Allerød (14–12.9 ka BP), Younger Dryas (12.9–11.7 ka BP) (Rasmussen et al., 2006)— and most of the Holocene (11.7–0.8 ka BP). All modelled ages and depths for Tramacastilla samples, as well as their sedimentation rate, are indicated in **Supplementary Data 7**.

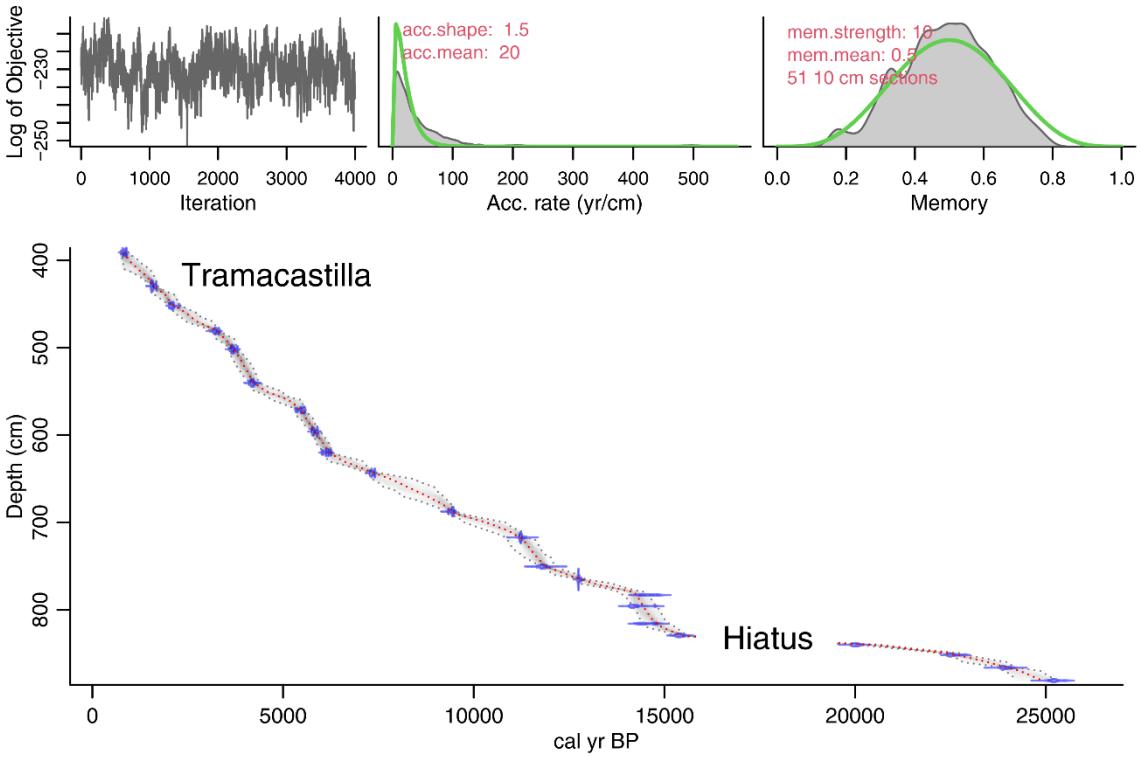


Figure 3: Bayesian age-depth model for Tramacastilla lacustrine sequence excluding sections 1U and 2U.

3.3 Vegetation dynamics and associated fire regime

Pollen samples span between 0.8 and 24.7 ka BP. On average, 439.1 ± 61.1 pollen grains were counted per sample, identifying a total of 108 terrestrial pollen types, with a mean of 28.7 ± 8.3 pollen types per sample (**Table C1**). **Figure 4** presents a selection of pollen groups that occur throughout the record and are representative of the major plant communities. Complete diagrams of pollen percentages and PARs for all pollen types are provided in **Figs. C1-4** and all pollen counts and PARs are included in **Supplementary Data 2** and **3**.

Charcoal analysis (**Fig. C5** and **Fig. 5b-d**) was restricted to the Holocene section of the sequence. Accordingly, the charcoal samples are dated between 0.8 and 11.5 ka BP, with a mean temporal resolution of 31.5 ± 18.9 years per analysed sample. Charcoal counts ranged from 0 to 83, with a mean of 6.3 ± 7.4 charcoal particles per sample, and a mean of 0.23 ± 0.37 mm^2 (**Table C1**). CHAR (**Fig. 5b**) oscillates between 0 and 32926, with mean of 2298 ± 3017 $\mu m^2 \cdot cm^{-2} \cdot yr^{-1}$, and the W/L ratio (**Fig. 5c**) has a mean value of 0.55 ± 0.26 (**Table C1**). A total of 16 fire episodes have been detected along the record (**Fig. 5c**), with a mean FRI of 376 years between two consecutive fire events, and a maximum value of 1200 years between fire events is reached ca. 6.2 ka BP. There is a low correlation between CHAR and sedimentation rate (Spearman correlation coefficient = 0.28). This indicates that sedimentary processes may have low influence on charcoal accumulation in Tramacastilla lake. All charcoal metrics are included in **Supplementary Data 4**.

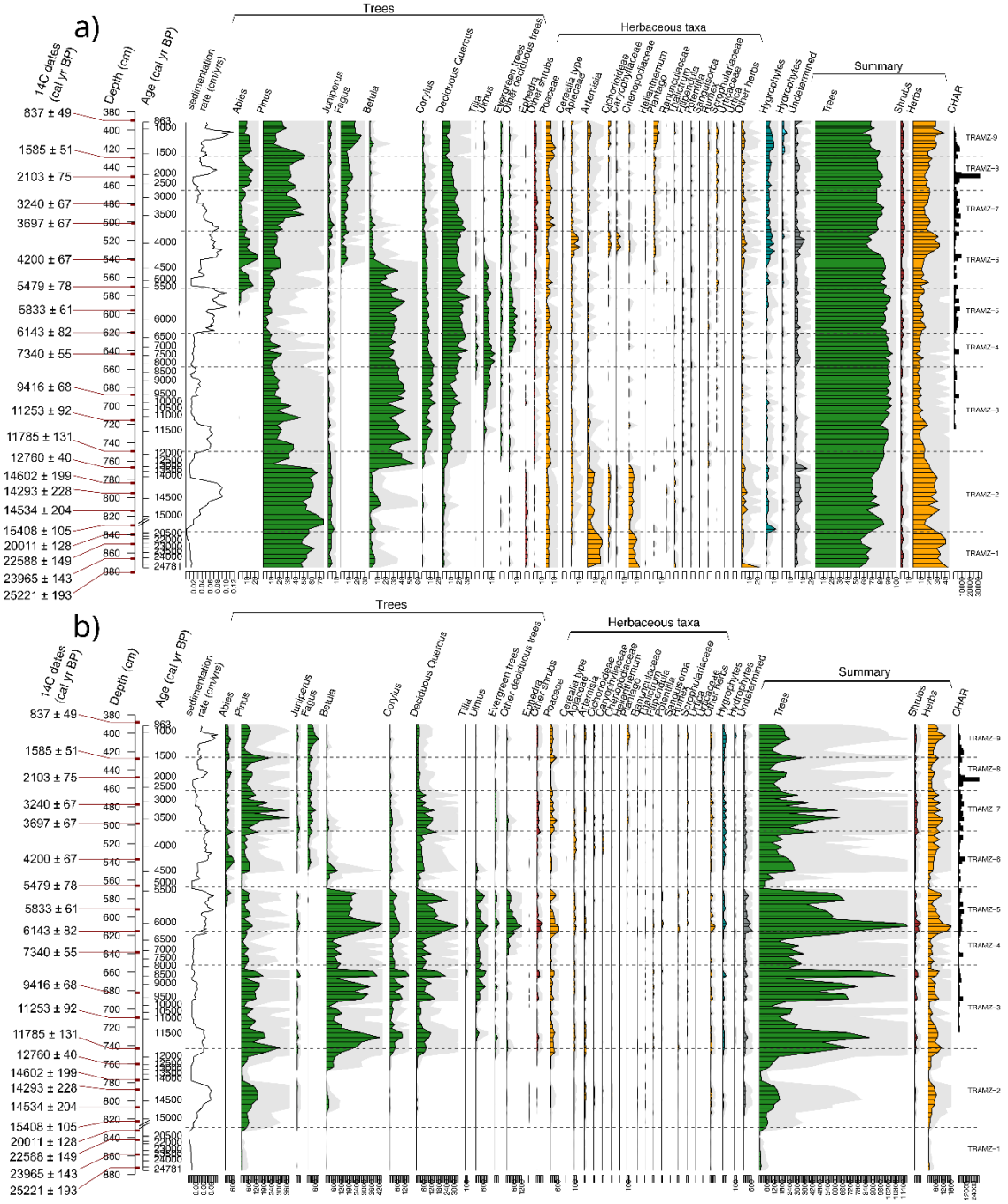


Figure 4: Pollen diagrams of TRAM: a) in percentages, b) in PAR (pollen grains·cm-2·yr-1). CONISS-made zones are separated with dashed lines (TRAMZ-1 to 9), sedimentation rate (cm/yrs) spectrum is on the left, and CHAR ($\mu m^2 \cdot cm^{-2} \cdot yr^{-1}$) on the right. Green is used for trees, dark red for shrubs (*Ephedra* and other shrubs), orange for herbaceous taxa, dark blue for hygrophytes, light blue for hydrophytes and grey for undetermined pollen types.

Nine vegetation zones have been identified from the constrained cluster analysis (CONISS) of PAR (TRAMZ-1 to 9, **Fig. 4**):

- TRAMZ-1 (876-834 cm depth; 25-17.9 ka BP): this first zone starts with both low sedimentation rate and PARs for all taxa, reflecting reduced plant productivity. *Pinus* stands out as the main arboreal taxon, with 45-65% abundances while other woody taxa (e.g. *Juniperus, Betula*) appear low (0-10% cover). Poaceae, *Artemisia* and Chenopodiaceae are the next most abundant taxa both in frequency and PAR, especially *Artemisia*, with values ca. 20%. The end of the zone (between 840 and 830 cm depth), corresponds to the sedimentary hiatus.
- TRAMZ-2 (834-747 cm depth; 17.9-11.8 ka BP): this zone records increasing sedimentation rate, resulting in higher PARs, where *Pinus* stands out as the dominant taxon both in relative abundance and biomass, reaching its maximum percentage (75%) at the beginning of the zone. Among arboreal taxa, only *Betula* shows a biomass and percentage peak ca. 14.5 ka BP, and *Juniperus* shows continuous values around 5% though low biomass. Herbaceous taxa such as Poaceae, *Artemisia,* Apiaceae or Chenopodiaceae remain constant in the landscape, recording a notable biomass increase ca. 14.5 ka BP. At the end of this zone, sedimentation rate decreases as well as *Pinus*, *Artemisia*, Cichorioideae and Chenopodiaceae frequencies, while other taxa (e.g. *Betula*, *Corylus*, deciduous *Quercus* and Poaceae) increase, including their biomass, indicating the onset of deciduous forest development. Over this period, *Betula* dominates the canopy, outcompeting *Pinus* in relative abundance and reaching its highest values in the entire record.
- TRAMZ-3 (747-656 cm depth; 11.8-8.2 ka BP): at the Holocene onset, the mixed forest prevails. *Betula* dominates the deciduous community, where *Quercus*, *Corylus*, *Ulmus* and to a lesser extent *Tilia*, co-occur. These taxa show high PARs except for the period between 11.2-9.8 ka BP, where their biomass reduces, to later increase. *Pinus* peaks early, then declines both in biomass and relative abundance throughout the zone. Herbaceous taxa show low and constant PARs and decreasing percentages. CHAR (**Fig. 5b** and **Fig. C5**) exhibits a steady background input with several peaks and four fire events (**Fig. 5c**), reflecting a constant fire occurrence in Tramacastilla. A mean W/L ratio < 0.5 during this period suggests that the main fuel were grasslands (**Fig. 5d** and **Fig. C5**).
- TRAMZ-4 (656-618 cm depth; 8.2-6.2 ka BP): the sedimentation rate during this zone remains low and constant, with values around 0.02 cm/yr. Coinciding with the beginning of the Mid-Holocene (Northgrippian) at 8.2 ka BP, an abrupt and sustained biomass decrease is recorded for woody (e.g. *Pinus*, *Betula*, *Corylus*, deciduous *Quercus*, *Ulmus*) and herbaceous plants (e.g. Poaceae, Apiaceae). Meanwhile, pollen percentages remain similar to the previous zone for woody taxa, with slight decreases in *Betula*, *Corylus* and *Ulmus*, and an increase in deciduous *Quercus*. During this zone *Fraxinus* appears for the first time in the record (**Fig. C1**). Fire activity during this period is lower than the previous zone, with a low CHAR background and only one fire episode, while W/L ratio remains < 0.5, suggesting grass burning.
- TRAMZ-5 (618-569 cm depth; 6.2-5.5 ka BP): a pronounced increase in the sedimentation rate accompanies a biomass increase in woody (e.g. *Betula*, *Corylus*, deciduous *Quercus*, *Ulmus* and other deciduous trees) and to a lesser extent in herbaceous plants (e.g. Poaceae, Apiaceae, *Rumex*) and hygrophytes. Evergreen trees present their maximum biomass values; the deciduous forest prevails dominant in the landscape while *Pinus* shows its lowest percentages of

the record (ca. 10%). This zone records the expansion of *Abies* ca. 6 ka BP, showing similar trends both in PARs and frequencies. *Fagus* lowly appears at the end of the zone (5.6 ka BP). Fire dynamics exhibit larger background signals than before, with a concentration of several fire events, and the W/L ratio still indicates herbaceous fuel.

- TRAMZ-6 (569-508 cm depth; 5.5-3.8 ka BP): sedimentation rate drops at the beginning of this zone, causing a sharp decline in plant biomass across all taxa. A later increase shows biomass recovery of woody taxa (*Abies*, *Pinus* and deciduous *Quercus)*, while *Betula* and *Ulmus* continue to decline, marking the collapse of *Betula*-dominated forest by the zone's end. Around 4.5 ka BP, *Fagus* expands both in biomass and relative abundance. Herbs keep low biomass, though some taxa record an increase in frequency at 4.2 ka BP (Apiaceae, Cichorioideae, Caryophyllaceae, *Plantago*), as well as hygrophytes. CHAR drops to the lowest background in the sequence with some peaks and two fire episodes, and a shift towards increased woody fuel is indicated by the W/L ratio.
- TRAMZ-7 (508-463 cm depth; 3.8-2.7 ka BP): the decreasing sedimentation rate, contrasts with the increasing *Pinus* frequency (50%) and biomass, reaching its maximum recorded values. Meanwhile, only deciduous *Quercus* prevails among broadleaved woody taxa (20%), and continuous PAR, alongside *Abies* and *Fagus* (oscillating around 10%). Poaceae show biomass expansion, and records higher frequencies than before, while other herbaceous plants show decreasing values (e.g. Apiaceae, Cichorioideae, Caryophyllaceae). Fire activity increases compared to the prior periods, with a rising CHAR background input, though only one fire event, and mainly woody plants burning.
- TRAMZ-8 (463-427 cm depth; 2.7-1.6 ka BP): this zone features a deciduous *Quercus* biomass decline, *Abies*-*Fagus* community increasing abundances and constant biomass, and pinewoods remaining present in the landscape, both in frequency and PARs. Herbaceous plants (e.g. Poaceae, Apiaceae, *Artemisia*, *Plantago*, Scrophulariaceae, other herbs) keep similar relative representation than previously, and low biomass. This zone exhibits the highest CHARs, (ca. 33000 $\mu m^2 \cdot cm^{-2} \cdot yr^{-1}$), ca. 2.1 ka BP. During this period, two fire episodes are detected, and the W/L ratio > 0.5 indicates predominantly burning of woody taxa, as it happened in the two previous periods.
- TRAMZ-9 (427-390 cm depth; 1.6-0.8 ka BP): the topmost pollen zone of Tramacastilla is defined by a starting peak in *Pinus* biomass and relative abundance to rapidly decrease. PARs remain similar to previous levels, indicating the dominance of *Abies*, *Pinus* and *Fagus*, which peaks in biomass around 1.1 ka BP. Deciduous *Quercus* is also present, though less abundant. In contrast, herbaceous taxa increase in biomass and relative abundance, particularly those associated with human activity (Cerealia type, *Plantago*), reaching their highest percentages. The record ends with decleaning CHAR, one fire event and a mean W/L ratio > 0.5, indicating predominantly woody vegetation burning.

3.4 *sed*aDNA analysis

A total of 423 plant and 62 animal taxa have been identified in 46 sediment samples through *sed*aDNA analysis, dating between 12.2 and 1.3 ka BP (**Supp. Data 5 and 6**). A thorough discussion of methods and results for *sed*aDNA methods are described in Julián-Posada et al. (2025). We express these results as Relative Abundance Index (RAI) (Garcés-Pastor et al., 2022), that represents the proportion of DNA sequences assigned to a specific taxon relative to the total number of sequences in the sample

and the number of PCR replicates (see Rijal et al., 2021). This metric provides a standardised estimate of taxon abundance, allowing comparisons across samples with varying sequencing depths. Here, we present domestic animals' *sed*aDNA (**Fig. 5e**) and a synthesis of plant *sed*aDNA classified using the same taxonomic groups as the pollen data to support integrated interpretation (**Figs. 5, 6**).

4 Discussion

Vegetation reconstructions from Tramacastilla (TRAM) and other Pyrenean lacustrine records (Garcés-Pastor et al., 2017; González-Sampériz et al., 2006; Leunda et al., 2020; Pèlachs et al., 2007; Pérez-Obiol et al., 2012; Pérez-Sanz et al., 2013) suggest that climate was the main driver of vegetation dynamics at high altitudes of the Pyrenees at least until the Neolithic onset (7.5 ka BP), when the first palaeoenvironmental indicators of human impact emerge (Gassiot-Ballbè et al., 2017; Laborda, 2019). Our data provide new evidence challenging previous interpretations on human impact in the subalpine belt of the Southern Pyrenees. Indeed, there is no consensus on whether this human influence has had a noticeable effect on ecosystems from 7.5-5 ka BP onward (Ejarque et al., 2010; Pérez-Díaz et al., 2015; Revelles, 2017; Van Der Horst et al., 2024), or if its impact became evident and at a broader scale ca. 1 ka BP, when unequivocal anthropogenic indicators appear everywhere and at all altitudes (González-Sampériz et al., 2017, 2019). In section 5.1 we explore and compare the methodological approaches applied in our site, and in section 5.2, 5.3 and 5.4 the vegetation changes are interpreted and situated in a regional context.

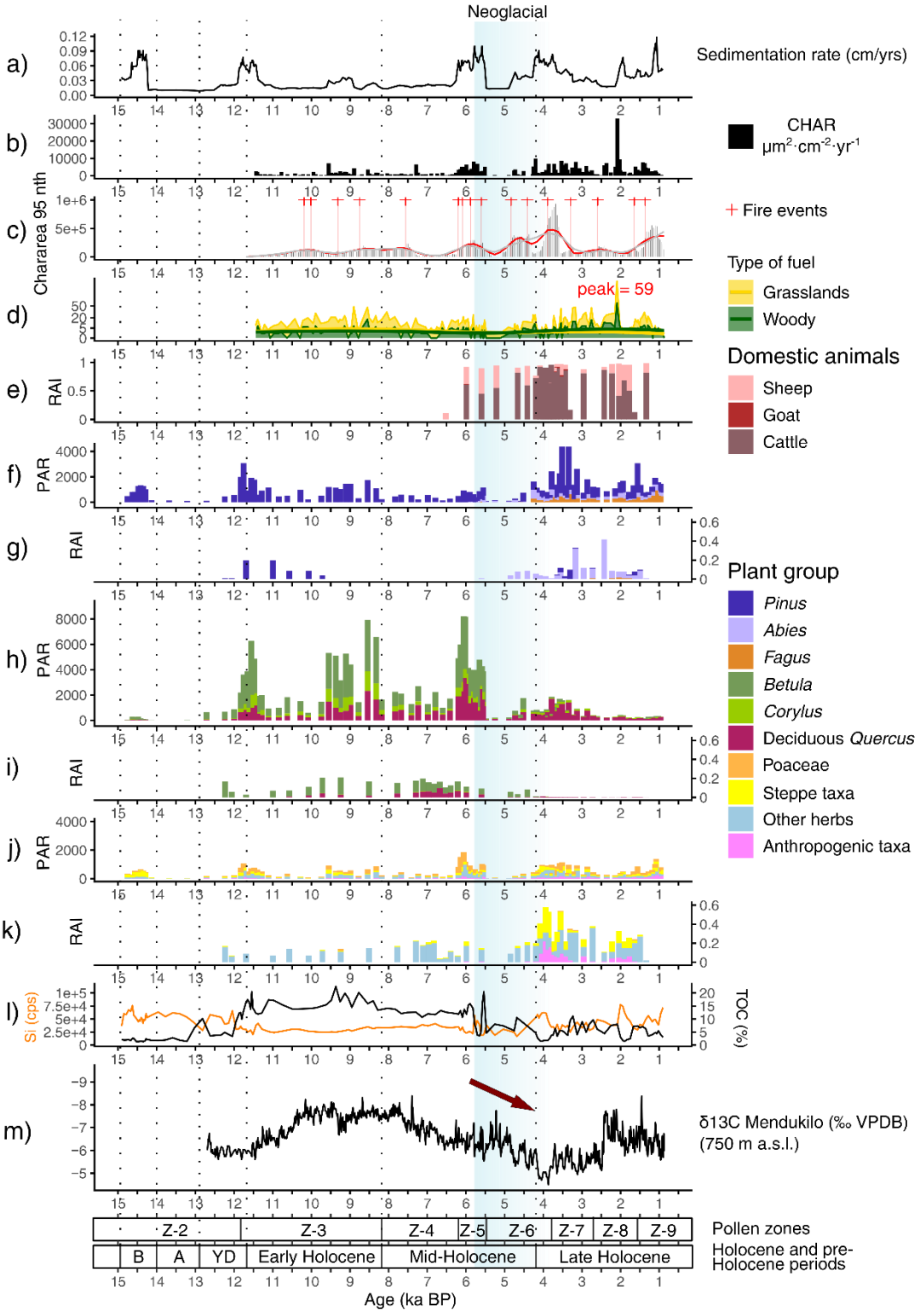

Neoglacial
a)
Sedimentation rate (cm/yrs)
b)
CHAR
µm²·cm⁻²·yr⁻¹
c)
Chararea 95 nth
Fire events
Type of fuel
Grasslands
Woody
d)
peak = 59
Domestic animals
Sheep
Goat
Cattle
e)
RAI
f)
PAR
g)
RAI
Plant group
Pinus
Abies
Fagus
Betula
Corylus
Deciduous Quercus
Poaceae
Steppe taxa
Other herbs
Anthropogenic taxa
h)
PAR
i)
RAI
j)
PAR
k)
RAI
l)
Si (cps)
TOC (%)
m)
δ13C Mendukilo (‰ VPDB)
(750 m a.s.l.)
Z-2
Z-3
Z-4
Z-5
Z-6
Z-7
Z-8
Z-9
Pollen zones
B
A
YD
Early Holocene
Mid-Holocene
Late Holocene
Holocene and pre-Holocene periods
Age (ka BP)

Figure 5: Tramacastilla's proxies synthesis and non-quantitative temperature reconstruction from Mendukilo cave: a) sedimentation rate (cm/yrs); b) CHAR ($\mu m^2 \cdot cm^{-1} \cdot yr^{-1}$); c) fire events; d) W/L ratio; e) RAI (Relative Abundance Index) for domestic animals;,f, h, j) PAR (number of pollen grains$\cdot cm^{-2} \cdot yr^{-1}$) for different vegetation types; g, i, k) *sed*aDNA (Relative Abundance Index-RAI) for the same vegetation types; l) selection of geochemical measurements (Si counts per second, TOC percentages); m) temperature reconstruction based on **δ**13C (‰ VPDB) for Mendukilo cave (Bernal-Wormull et al., 2023). Pollen zones (TRAMZ-2 to 9) are indicated at the bottom of the figure. Pre-Holocene periods (B: Bølling, A: Allerød, YD: Younger Dryas) (Rasmussen et al., 2006) and Holocene subdivisions (Walker et al., 2018) are indicated at the bottom of the figure, and separated with dashed lines. The Neoglacial period (García-Ruiz et al., 2020a) is shown in light blue. All colours are suitable for colour blindness.

4.1 Improved and more accurate vegetation dynamics through multi-proxies' comparison

We have applied and compared here two different datasets (three metrics) to reconstruct past vegetation from lake sediments, for the first time in the Iberian Peninsula: pollen percentages, PAR and *sed*aDNA expressed in RAI (**Fig. 6**). Vegetation reconstructions based on *sed*aDNA analyses have proven to have a local character (Giguet-Covex et al., 2019; Haile et al., 2007; Parducci et al., 2017; van Vugt et al., 2022), compared to those based on pollen analyses, that are known to reconstruct landscapes at a regional scale (Parducci et al., 2019). Nevertheless, it is important to note that there is currently no quantitative metric for taxa abundances in ancient DNA nor *sed*aDNA data (Alsos et al., 2016), precluding direct comparisons between fossil pollen and environmental DNA generally speaking. Despite the differing sampling resolutions between pollen and *sed*aDNA analyses at Tramacastilla, this comparison reveals several noteworthy patterns:

1) Although anthropogenic taxa (Cerealia type, *Plantago*, *Plantago* t. *media/major*, *Rumex* and *Urtica*) appear consistently throughout the pollen record—both in percentages (**Fig. 6a**) and PARs (**Fig. 6b**) —the *sed*aDNA data (**Fig. 6c**) reveal a more nuanced pattern, with these taxa first emerging around 6 ka BP and increasing notably after 4.5 ka BP. This discrepancy highlights the limitations of pollen analysis, where low taxonomic resolution often necessitates grouping diverse taxa under broad anthropogenic categories (e.g. *Trifolium* type). As a result, taxa not directly linked to human activity may be misclassified, potentially leading to an overestimation of human impact. In contrast, the higher taxonomic resolution of *sed*aDNA enables the identification of specific species associated with anthropogenic environments, such as *Trifolium pratense*, thereby offering a more accurate reconstruction of human influence on mountain ecosystems (Giguet-Covex et al., 2014).
2) Notably, *sed*aDNA from herbs (Steppe taxa and other herbs) is relatively more abundant than their corresponding pollen, particularly from ca. 4 ka BP, coinciding with the opening of the landscape in TRAM (Julián-Posada et al., 2025). This may reflect the highly localised nature of *sed*aDNA signals, whereby plant species growing in close proximity to the lake are potentially better represented than the regional flora—a pattern also observed in modern soil DNA studies (Alsos et al., 2018; Yoccoz et al., 2012).
3) Counterintuitively, Poaceae show a different scenario compared to other herbs: it is less represented in the *sed*aDNA record than with pollen. This is consistent with the known overrepresentation of Poaceae pollen in pollen records due to its high pollen productivity and wind dispersal, whereas Poaceae biomass is often relatively low and does not always amplify efficiently, which has been also seen in modern DNA studies (Alsos et al., 2018). While we might assume an overrepresentation of palatable herbaceous taxa through *sed*aDNA analysis due to their abundance in

animal droppings, our results point to the opposite scenario, where Poaceae, that groups most of grazed plants, is underrepresented. This suggests that, at least in our record, excrements do not appear to constitute a major source of the *sed*aDNA signal, although we cannot entirely exclude some contribution from this pathway.

4) Some arboreal taxa (e.g. *Betula, Abies*) display concurrent PAR and RAI results, while pollen percentages seem to have a different trend.
5) Other arboreal taxa (e.g. *Pinus, Fagus, Corylus,* deciduous *Quercus*) show lower RAI compared to pollen percentages, which may reflect their higher pollen productivities, and/or their absence in the lake surroundings.

Overall, the differences between the two proxies may be attributed on the one hand to varying pollen productivity and dispersal among taxa. On the other, altitude may play a role as the high elevation of Tramacastilla (1682 m a.s.l.) could imply that pollen rain is dominated by long-distance transported anemophilous taxa, resulting in broader-scale reconstructions (Ortu et al., 2006). Despite these differences in spatial resolution, the results underscore the complementarity of *sed*aDNA and pollen analyses in reconstructing both local and regional vegetation dynamics (Garcés-Pastor et al., 2022; van Vugt et al., 2022). In addition, they also point to the need for greater effort in researching the taphonomy of *sed*aDNA in order to improve vegetation reconstructions, and to consider PAR to better frame vegetation productivity.

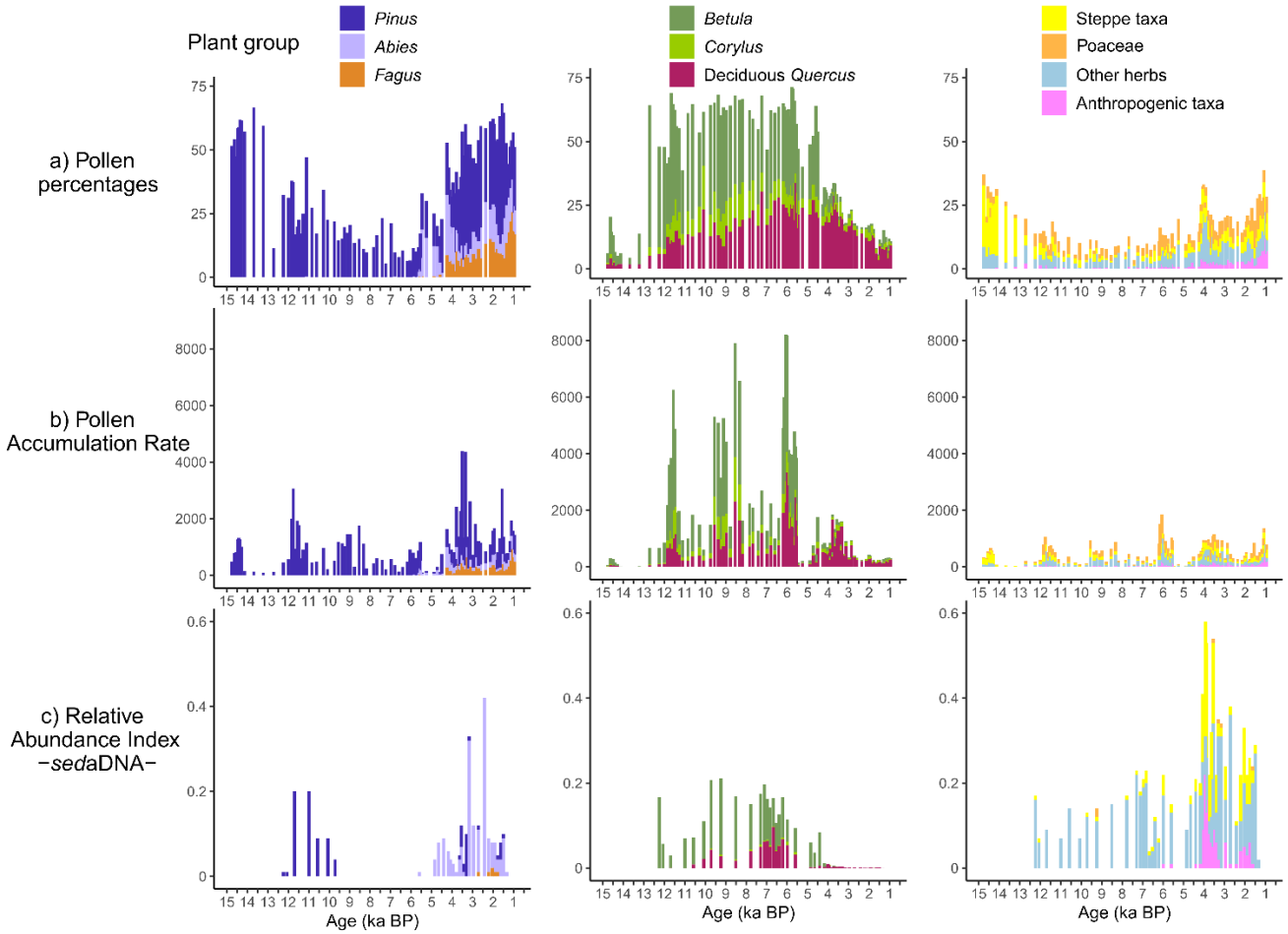


Figure 6: Comparison of the different methods and metrics used to reconstruct past vegetation in Tramacastilla lake: a) Pollen percentages (%); b) Pollen Accumulation rate (PAR, number of pollen grains·cm^{-2}·yr^{-1}); c) *sed*aDNA results expressed in Relative Abundance Index (RAI).

4.2 Lateglacial vegetation dynamics (25-11.7 ka BP)

The low sedimentation rate (**Fig. A2**) and the sedimentary hiatus at the beginning of the record (25-14.9 ka BP in 879-819 cm), as well as the low number of pollen samples available for this period (11) due to this rate, prevent us from accurately reconstructing the palaeoenvironmental conditions around TRAM. The abrupt change in sedimentation rate between 20-15 ka BP and the radiocarbon dates in this depth indicate a sedimentary hiatus (**Fig. A1**). In general terms, the reduced organic content, the high external sediment input and the high grain size of the sediment point to a low productivity lake under a glacial environment. The presence of pollen from taxa associated with cold conditions (*Pinus*, *Artemisia*, *Ephedra*, Chenopodiaceae) support this scenario, and coincides with other Pyrenean glacial deposits and records from the same chronological period (González-Sampériz et al., 2005), and lacustrine sequences such as El Portalet (González-Sampériz et al., 2006) or Pllan d'Están (Vidaller et al., 2024) (**Fig. 1**). More specifically, the increase of Asteroideae liguliflora (Cichorioideae) next to

Artemisia and Chenopodiaceae decrease at ca. 21 ka BP (**Fig. 4a**) suggests a shift towards less arid conditions, as it has been suggested for North-Eastern palynological sequences in previous glacial phases during the early and middle Pleistocene (González-Sampériz et al., 2010), illustrating the abrupt climatic oscillations that characterize the end of the Last Glacial Maximum-LGM and the subsequent Lateglacial period (González-Sampériz et al., 2017). These results also align with previous works from Tramacastilla (Garcia-Ruiz and Valero-Garces, 1998; Montserrat, 1992), that reveal a treeless landscape and hydrological fluctuations during the Lateglacial onset (prior to 14.5 ka BP). Given the low biological data for this period, no more detailed reconstruction is possible, so we have focused our discussion on the results for the end of the Lateglacial and mostly the Holocene (14.9-0.8 ka BP) (**Figs. 5, 6, 7**).

The onset of the Bølling (818-777 cm depth; 14.9-14 ka BP) is marked by the well-known rapid deglacial warming at a global scale, contrasting with preceding cold conditions (Ausín et al., 2024; Moreno et al., 2014; Rasmussen et al., 2006). Radiocarbon dates between 14.3-14.6 ka BP in TRAM are not consecutive, limiting the precise chronological placement of sedimentary processes during this interval (**Fig. A1**). In general terms, the low plant biomass, the dominance of steppe taxa at a regional scale independently of altitude (González-Sampériz et al., 2006, 2017; Vidaller et al., 2024), the high values of *Pinus* pollen proportions, and its co-occurrence with taxa such as *Juniperus*, *Ephedra*, *Artemisia*, Chenopodiaceae and Poaceae (**Fig. 4**), suggest an open landscape around the lake with scattered *Pinus* formations under cold conditions, unfavorable for the development of diverse plant communities. This coincides with a previous palynological study (Montserrat, 1992), where steppe herbs accompanied by *Pinus* would have dominated the vegetation. Sedimentologically, the Bølling corresponds to Unit 5 (**Fig. 2**), characterised by sediments supplied by runoff processes in a glacial environment (**Table B1**), consistent with a sparsely vegetated environment dominated by plants adapted to extreme conditions. The transition to the Allerød period (777-765 cm depth; 14-12.9 ka BP) implied lower biomass for all taxa, especially for *Pinus*, that abruptly declined (**Fig. 5f**). This period exhibits shifts in sedimentation and geochemical elements (Subunit 4e, **Fig. 2**), indicating increased lake productivity, that, despite the reduction of plant productivity, would underscore a shift towards more favourable climatic conditions compared to the Bølling. This transition is reflected in vegetation dynamics at a regional scale, especially in the subalpine belt of the Pyrenees, such as Tramacastilla, Pllan d'Están (Vidaller et al., 2024) and El Portalet (González-Sampériz et al., 2006) sequences. They record a decreasing trend in steppe taxa proportions, while deciduous trees expand, underscoring a change from cold and arid towards warmer and moister climatic conditions associated with the Allerød. Indeed, this trend has been also identified in other records from the Iberian Peninsula (Morellón et al., 2009; Sánchez-Morales et al., 2022; Van Der Horst et al., 2024), while in contrast other European records show a different tendency, with warmer conditions during the Bølling and decreasing temperatures during the Allerød (Lotter et al., 2012). This different trend could be due to a rapid increase in sea surface temperature in the western Mediterranean basin (Cacho et al., 2001), which would cause these humid conditions in southern Europe, though would not reach other parts of central or northern Europe.

The Younger Dryas (YD) (765-739 cm depth; 12.9-11.7 ka BP) is known to be a cooling period in the Northern Hemisphere (Rasmussen et al., 2006). In the Iberian Peninsula, hydrological responses during this interval were complex, resulting in two distinct climatic phases (Bartolomé et al., 2015): an initial dry phase (12.9-12.5 ka BP), followed by a humid phase (12.5-11.7

ka BP). In TRAM, the Younger Dryas corresponds to Subunit 4d (**Fig. 2**), which shares sedimentary facies with Unit 5, and records an important shift of TOC values (**Fig. 5l**). This change concurs with declining temperatures according to Mendukilo (**Fig. 1**) reconstruction (Bernal-Wormull et al., 2023; **Fig. 5m**), which indicates a return to glacial conditions. However, the low sedimentation rate (**Fig. 5a**) and the resulting low pollen resolution during the beginning of the YD do not evidence a clear vegetation response to a potential climate hardening, nor the ability to clearly distinguish the two hydrological phases in the principal plant communities. In fact, palynological sequences from the southern Pyrenees, either do not record the YD due to glacial advance or a constant period with a frozen lake surface (González-Sampériz et al., 2006; Leunda et al., 2017), or record patchy and heterogeneous vegetation landscapes around this period, shaped by local microenvironments (González-Sampériz et al., 2017). Chronological interpretation, besides, remains limited during this interval because of the "plateau effect" in radiocarbon dates (**Fig. 2**). Despite these limitations, it is worth mentioning that the presence of some deciduous taxa in the TRAM pollen record during this time (e.g. deciduous *Quercus*, *Corylus*, though not in the *sed*aDNA data), as well as in other nearby sequences, suggest the presence of regional refugial areas where these taxa would have persisted during glacial periods (García et al., 2022; González-Sampériz et al., 2017). This scenario aligns with findings from other Iberian records (Carrión et al., 2010; González-Sampériz et al., 2010; Moreno et al., 2011; Muñoz Sobrino et al., 2004; Ruiz-Alonso et al., 2019), reinforcing the role of southern Europe, including its continental interior, as a biodiversity hotspot and niche of climate refuges.

4.3 Subalpine landscape evolution in the Southern Pyrenees during the Early to Mid-Holocene (11.7-4.2 ka BP)

4.3.1 The Early Holocene (11.7-8.2 ka BP)

The Early Holocene (Greenlandian, 739-658 cm depth; 11.7-8.2 ka BP) begins with a rapid deglacial warming due to an increase in temperatures in the Northern Hemisphere (Ausín et al., 2024; Renssen et al., 2009), as well as in northeastern Iberia (i.e., Bernal-Wormull et al., 2023: **Fig. 5m).** In TRAM, this period is marked by a shift towards the most organic and productive part of the sediment (Subunits 4c, b, **Fig. 2**), indicating the development of a deeper lake system. This hydrological change reinforces the well-documented transition to warmer and wetter conditions at the Holocene onset in Europe (Rasmussen et al., 2007; Roberts et al., 2004). These conditions facilitated the expansion of temperate taxa replacing *Pinus* in southern European vegetation landscapes, particularly in Atlantic-influenced regions of the Iberian Peninsula (González-Sampériz et al., 2005; Morellón et al., 2018; Moreno et al., 2011; Sánchez-Morales et al., 2022). In the central-eastern Pyrenees, several records reflect less oceanic conditions, with the persistence and dominance of *Pinus*, alongside deciduous taxa, such as in Basa de la Mora (Pérez-Sanz et al., 2013), Marboré (Leunda et al., 2017), Bassa Nera (Garcés-Pastor et al., 2017) (**Fig. 7**), Bosc dels Estanyons (Miras et al., 2007) or Estanilles (Pérez-Obiol et al., 2012). In contrast, the current pollen-based vegetation reconstruction from TRAM sequence, supported by *sed*aDNA data and the previous palynological study (Montserrat, 1992), reveals a transition from Lateglacial *Pinus* communities into a mixed forest dominated by *Betula* (**Figs. 6, 7**), with a general increase of plant biomass compared to the Lateglacial (**Fig. 6b**). This pattern would reflect humid conditions and/or a westward shift of the Atlantic-Mediterranean bioclimatic boundary. This dominance of *Betula* in TRAM, compared to other taxa, is not

recorded in other sequences, where *Corylus* usually is the major deciduous taxa in relative frequencies (Gil-Romera et al., 2014; González-Sampériz et al., 2006; Leunda et al., 2017), or both *Betula* and *Corylus* coexist in similar abundances (Garcés-Pastor et al., 2017) (**Fig. 7**). Only in Basa de la Mora (Leunda et al., 2020; Pérez-Sanz et al., 2013), higher percentages of *Betula* over *Corylus* are recorded, although *Pinus* is the dominant taxa. In the Alps, different studies have evidenced that higher fire frequencies favour the abundance of woody taxa with some sort of post fire response, as *Corylus* and *Betula* (Tinner et al., 2000). However, in the Pyrenees *Betula* has been proven to be negatively affected by fires in the first 150 years after the fire event (Gil-Romera et al., 2014). Considering these scenarios, we propose that, in TRAM, regular low intensity fires throughout the Early Holocene (**Fig. 5b, c**), would have encouraged *Betula* to dominate and expand at the expense of *Corylus*, owing to its advantage in disturbed, pioneer habitats (Pausas and Paula, 2012). This hypothesis is also supported by: 1) a similar situation in Basa de la Mora with higher percentages of *Betula* and a low fire activity (Leunda et al., 2020); 2) the absence of fires during the Early Holocene in Basa Nera (Garcés-Pastor et al., 2017), that would have equally favoured both *Corylus* and *Betula*; and 3) the higher presence of *Corylus* in El Portalet and Marboré (Gil-Romera et al., 2014; Leunda et al., 2017), that would be explained by a higher pollen input from the wetter northern slope of the Pyrenees, where *Corylus* is more abundant than *Betula* (Rius et al., 2009, 2011).

The rapid development of temperate forests during the Early Holocene is consistent with the establishment of favourable climatic conditions. However, this pattern alone does not demonstrate the existence of regional glacial refugia. Similar rapid afforestation also occurred in areas of Central Europe without nearby refugial populations. Nevertheless, our results are compatible with the previously exposed idea about the existence of regional glacial refugia in inner northeastern Iberia (García et al., 2022; González-Sampériz et al., 2010), likely located at intermediate elevations of the Pyrenees or even in the lowlands of the Ebro basin (González-Sampériz et al., 2004; Valero-Garcés et al., 2000). The varying abundance of *Betula* or *Corylus* in different Pyrenean sequences could also be explained by the proximity of species-specific refuge areas. In the particular case of TRAM, the Gállego River valley could have acted as a crucial dispersal corridor, facilitating the expansion of *Betula* from nearby refuge areas along the valley. Additionally, differences in dispersal strategies could have lead to this distributional pattern, as the winged fruits of *Betula* are more easily dispersed than heavy hazelnuts of *Corylus.* This *Betula* expansion may have been further promoted by fire activity, which creates open landscapes favourable for this taxa, resulting in the recorded scenario for Tramacastilla lake.

The high biomass recorded in TRAM at the end of the Early Holocene (9.7-8.2 ka BP), with maximum values at 8.5 ka BP (**Fig. 6b**), also indicates that more fuel would be available for burning (Kaltenrieder et al., 2010; Pausas and Paula, 2012). This would explain the continuous occurrence of fires, and the increment of CHAR recorded since 9.5 ka BP (**Fig. 5b**), with several fire episodes identified since ca. 10 ka BP (**Fig. 5c**). This pattern concurs with other Pyrenean sites, where regular fire occurrence is recorded during the Early Holocene (**Fig. 7**) (Gil-Romera et al., 2014; Leunda et al., 2020; Rius et al., 2012). As suggested by W/L ratio (**Fig. 5d**), more herbaceous taxa would be burning during the Early Holocene, even though there was a dominance of forest ecosystems. This apparently paradoxical scenario may be explained by the occurrence of frequent, probably natural, but low intensity fires (e.g. ground fires instead of crown fires), that would have prevented trees from

massively burning (Power et al., 2008). Nevertheless, the absence of W/L data for other Pyrenean sequences preclude us from knowing whether these results are generalisable for that period or are limited to the particularities of the Tramacastilla context.

4.3.2 The Mid-Holocene (8.2-4.2 ka BP)

The 8.2 ka cooling event marks the onset of the Mid-Holocene (Northgrippian, 658-538 cm depth, 8.2-4.2 ka BP, Walker et al., 2018). While this event is not evident in the TRAM sedimentation (**Fig. 2**) or pollen percentages (**Fig. 7**), it is marked by a pronounced decline in the biomass of deciduous trees, *Pinus* and herbaceous plants (**Fig. 5f, h, j**), alongside a reduction in CHAR (**Fig. 5b**), and a consequent absence of fire events until ca. 7.5 ka BP (**Fig. 5c**). Our hypothesis is that these changes reflect cold, arid conditions that reduced biomass and thus fuel availability. The absence of a clear signal in the relative abundance of vegetation is likely due to low sampling resolution around this event (no pollen samples between 8.2 and 7.8 ka BP). Pyrenean records exhibit complex responses to the 8.2 ka event: some sequences from high altitudes of Spanish Pyrenees such as El Portalet (González-Sampériz et al., 2006) and Basa de la Mora (Pérez-Sanz et al., 2013) (**Fig. 7**), as well as Lourdes in the French slope (Rius et al., 2012), indicate cool and dry conditions with a general decrease of deciduous trees. In contrast, other easternmost and/or lowland sites reflect warmer winters and increased humidity (González-Sampériz et al., 2017; Pla and Catalan, 2005). This discrepancy may arise from climatic differences, with Atlantic-influenced sites (e.g., El Portalet and Lourdes) showing stronger responses compared to those under Mediterranean conditions or capturing both bioclimatic influences, that seem not to be intensively affected by this event. This spatial discrepancy in the climatic signal likely explains the variable ecological responses. The climatic complexity during the 8.2 ka event is mirrored by a stark contrast in human socio-ecological systems: intense aridity appears to have driven the abandonment of harsh Mediterranean lowlands, such as the Bajo Aragón region. Conversely, the Pyrenean lowlands exhibit remarkable resilience, with human occupations showing continuity without evidence of migration (Alday et al., 2018; González-Sampériz et al., 2009; Montes et al., 2016). This juxtaposition underscores a complex scenario for the 8.2 ka event in the patched vegetation landscape of southern Europe.

The sediment continues with organic-rich sedimentary facies (Subunit 4a, **Fig. 2**), reflecting persistent deep-lake conditions until ca. 6 ka BP. During this initial organic-rich phase between 8.2 and 6 ka BP, where TOC reaches 20% (**Fig. 5l**), there is a prevalent dominance of *Betula* and deciduous *Quercus* communities in dominating the landscape (**Fig. 5h, i**). This sustained presence of deciduous *Quercus*, in contrast to other Pyrenean sequences (**Fig. 7**), could be explained by the lower altitude of Tramacastilla, as deciduous *Quercus* found in the Pyrenees are species characteristic of sub-Mediterranean environments (i.e., *Q.faginea, Q.humilis, Q.pubescens*) and these bioclimatic conditions would have reached TRAM during the Holocene (Jalut et al., 1997). During this period, the Mendukilo cave δ13C record shows the beginning of a continuous decline in temperature after remaining stable since 10 ka BP (Bernal-Wormull et al., 2023) (**Fig. 5m**), whereas chironomid temperature reconstruction from Basa de la Mora (Tarrats et al., 2018) shows constant and high summer temperatures until 6.2 ka BP. The vegetation reconstruction from TRAM, especially the continuous presence of *Betula*, seems to underscore favourable climatic conditions and high humidity, as evidenced in other Iberian and Pyrenean sequences, that record during the Mid-Holocene (Northgrippian) the greatest forest development (Carrión et al., 2010; González-Sampériz et al., 2017; Leunda et al., 2020; Pèlachs et al., 2007;

Pérez-Sanz et al., 2013). Furthermore, the presence of wild mammals such as red deer (*Cervus elaphus*) and bear (*Ursus arctos*) through *sed*aDNA analysis (Julián-Posada et al., 2025) during this period supports the scenario of a natural broadleaf forest where these animals would live without intense human hunter pressure, as no human evidence is identified through pollen or *sed*aDNA data over this time (**Fig. 6**).

The fire regime at TRAM between 8.2-6.2 ka BP suggests low fire activity with only one fire event at ca. 7.5 ka BP (**Fig. 5c**), which aligns from nearby El Portalet, where no clear fire events are identified between 7.7-6 ka BP despite the presence of charcoal particles (Gil-Romera et al., 2014). Other Pyrenean sequences record low fire activity during this period too, such as Marboré, Basa de la Mora (**Fig. 7**) (Leunda et al., 2020), Lourdes (Rius et al., 2012), Basa Nera (Garcés-Pastor et al., 2017) and the eastern Pyrenees (Cunill et al., 2013). Although Neolithic humans were present at a regional scale in lower altitudes, such as Chaves cave since 7.3 ka BP (Sierra et al., 2019), it does not seem feasible that the low fire activity in TRAM was human-driven looking the openness of the landscape, as no anthropogenic indicators nor domestic animals (**Fig. 5e**) are found through *sed*aDNA until 6.5 ka BP (Julián-Posada et al., 2025). Thus, this situation points to natural fires that could have been influenced by a Mediterranean climate regime during this period, with wet winters and relatively drier summers (Jalut et al., 1997), implying summer thunderstorms triggering natural blazes. Indeed, the fires identified in TRAM and comparable sequences during this interval (**Fig. 7**) (Leunda et al., 2020) may have been low in intensity and restricted in spatial extent, driven by localised factors that failed to influence neighbouring sites.

Between 6-4 ka BP, a gradual temperature decrease is evidenced in Mendukilo Cave (Bernal-Wormull et al., 2023) (**Fig. 5m**). This climatic shift towards cooler conditions, also known as the Neoglacial period, has already been identified in higher altitudes of the central Pyrenees (García-Ruiz et al., 2020a; Leunda et al., 2019). In the TRAM sequence, alternating runoff-dominated sedimentary layers appear at ca. 6 ka BP (Subunit 3f, e, **Fig. 2**), suggesting erosive processes in the lake surroundings, pointing to a less forested environment due to unfavourable climatic conditions or increased human pressure. These variations coincide with the first evidence of domestic animals —cattle and sheep— in the TRAM record around 6.5-6 ka BP (**Fig. 5e,** Julián-Posada et al., 2025), that persist around the lake throughout the rest of the sequence. Concurrent vegetation changes are also recorded, as revealed by pollen and *sed*aDNA analyses, with a gradual decrease of plant productivity for all taxa, reaching minimum PARs (**Fig. 6b**), and the appearance of novel herbaceous taxa (Julián-Posada et al., 2025). Ultimately, all these evidence point that human activity contributed to landscape opening to create suitable environments for grazing (Ejarque et al., 2009; Rius et al., 2012; Schwörer et al., 2015), and then, increase of erosion and a high concentration of fire episodes at ca. 6 ka BP (**Fig. 5c**) existed. Indeed, the concurrence of these fire episodes with the lowest temperature reconstruction in Mendukilo (**Fig. 5m**) supports a scenario of human-driven fires. However, these fires would have a local character, as their effect is not reflected in the pollen spectra but in the *sed*aDNA record (**Fig. 5g, i, k**). Consequently, it seems unlikely that human activity alone was responsible for the general landscape opening observed both in regional and local plant proxies. Instead, we propose that our record reflects a synergistic effect between the activities of Neolithic pastoralists—aimed at creating open areas for grazing—and a broader climatic shift towards cooler conditions, which

likely promoted the expansion of open landscapes at the expense of forests. Pastoralist practices would have then further maintained these open areas by ensuring continued herbivore use.

The expansion of *Abies* around 6 ka BP, is evidenced in both pollen and *sed*aDNA records in TRAM (**Fig. 5f, g**), and occurred synchronously across the southern Pyrenees (**Fig. 7**). This takes place under the Neoglacial climatic conditions, consistent with the well-known arrival of this species following a post glacial expansion from coastal refuge areas (Pèlachs et al., 2009; Terhürne-Berson et al., 2004). The expansion of *Fagus*, later than *Abies*, concurs with the timing observed in other records at a regional to subcontinental scale (Garcés-Pastor et al., 2017; López-Merino et al., 2008; Magri, 2008; Pérez-Obiol et al., 2012; Pérez-Sanz et al., 2013; Rius et al., 2011). However, TRAM shows lower frequencies and PAR than the aforementioned studies until ca. 4.2 ka BP (**Fig. 5f**), indicating a more gradual establishment. While some studies attribute the development of both *Abies* and *Fagus* in Europe to anthropogenic drivers (Kozáková et al., 2011; López-Merino et al., 2008; Morales-Molino et al., 2022; Rey et al., 2019), others point to climate as the main driver, even highlighting the negative effect that anthropogenic activities have on them (Aregger et al., 2025; Pèlachs et al., 2009; van Vugt et al., 2022; Wick and Möhl, 2006), and on *Abies* in particular (Henne et al., 2013; Morales-Molino et al., 2021; Tinner et al., 2013). In the case of TRAM, the timing and synchronicity of the arrival of these species across the Pyrenees (**Fig. 7**) point to a large-scale climatic driver for their initial establishment. The arrival of *Abies* coincides with the onset of the cool and humid Neoglacial period in Central Pyrenees as evidenced by glacial moraines and ice cave deposits (García-Ruiz et al., 2020a; Leunda et al., 2019), conditions which are known to facilitate its expansion (Tinner and Lotter, 2006). *Fagus* has similar environmental requirements as *Abies*, although it is less drought-tolerant (Costa et al., 2005), so it could only expand when Atlantic conditions are more fully established, and therefore, later in the Holocene. Considering this evidence, we hypothesise that the expansion of both *Abies* and *Fagus* in TRAM was triggered by climatic conditions, and anthropogenic activities – intensified ca. 4 ka BP – may have subsequently facilitated their spread, providing a competitive advantage over previously dominant taxa.

Overall, we propose that both the Neoglacial climatic deterioration and human activities initiated a progressive contraction of forest cover and new dominant trees through grazing practices and deliberate fires continued this inertia, leading to increased landscape openness by approximately 4.5 ka BP (**Fig. 5k**). While herbaceous PARs remain low around 4 ka BP (**Fig. 5j**), *sed*aDNA reveals an abrupt local change between 4.5-4 ka BP, with herbaceous taxa reaching maximum RAIs (**Fig. 5k**). This is concurrent with increasing CHARs (**Fig. 5b**) and several fire events (**Fig. 5c**), suggesting maintained landscapes modified by humans. Although definitive evidence remains limited, our findings suggest a scenario in which cooler climatic conditions were followed by sustained human-driven forest decline, offering an alternative hypothesis that integrates both climatic and human drivers in shaping the TRAM landscape.

4.4 Drivers of today's vegetation and future directions for management: The Late Holocene (4.2-0.8 ka BP)

The Late Holocene (Meghalayan, 538-390 cm depth; 4.2-0.8 ka BP) exhibits sedimentation dynamics comparable to those of preceding periods (Subunits 3d-a, **Fig. 2**), though with notably lower TOC content (**Fig. 5l**), pointing to less biological productivity. Biomass declines across all plant taxa at the Late Holocene onset (**Fig. 6b**), and a reduction of CHAR is also

recorded (**Fig. 5b**), concurring with the so-called 4.2 ka event, regionally recorded in Mendukilo with the minimum Holocene temperatures (Ausín et al., 2024; Bernal-Wormull et al., 2023). The period after 4 ka BP records a gradual increase in temperatures (**Fig. 5m**), and is characterised by increased aridity across the Mediterranean (Araus et al., 1997; Di Rita et al., 2018), the Iberian Peninsula (Ausín et al., 2024), as well as in the Pyrenean region (González-Sampériz et al., 2017). Indeed, such aridity could be partly reflected in our pollen and *sed*aDNA records through the landscape openness (**Fig. 5k**), the regional biomass increase of *Pinus* (**Fig. 5f**) with its presence at a local scale (**Fig. 5g**), and the collapse of the mixed-deciduous forest during this interval, where only deciduous *Quercus* thrives (**Fig. 5h, i**). At ca. 2 ka BP, the highest CHAR is recorded (**Fig. 5b**), although it does not concur with a single fire episode (**Fig. 5c**), and might therefore be connected to the regional fire activity. This would explain the lack of a clear fire effect on local vegetation, as no responses are identified in the *sed*aDNA record (**Fig. 5g, i, k**). Indeed, this period corresponds to the Iberian-Roman humid period (2.6-1.6 ka BP), with humid and warm environmental conditions (Currás et al., 2012; Martín-Puertas et al., 2009) that would have facilitated both natural and human-made regional fire activity.

The sparsely distributed tree communities during the Late Holocene would have been partly composed by the *Abies–Fagus* forests, which had already become established by that time (**Fig. 5f, g**). While the regional landscape would have been shaped by *Pinus* and *Quercus* (**Fig. 5h, i**), the immediacy of TRAM would have been dominated by *Abies*, as revealed by *sed*aDNA (**Fig. 5g**). Regarding the herb layer, Poaceae and other herbaceous taxa are present with similar biomass than in previous periods, but herbs increase after 4 ka BP in the *sed*aDNA record (**Fig. 5k**), which would suggest a shift towards a more open landscape in the vicinity of TRAM despite low biomass.

The coexistence of forest communities and open ecosystems during the Late Holocene seems congruent with the disturbance dynamics observed in Tramacastilla. Since 4 ka BP, there is continuous presence of fires with either higher frequency, and/or severity, with woody plants as the primary fuel (**Fig. 5c, d**). The predominance of woody over herbaceous plant combustion during this period—despite the reduced tree biomass compared to previously (**Fig. 6**)—would suggest that fires were less frequent but of greater severity (Archibald et al., 2013; Power et al., 2008). This apparent shift from grassland to more tree-fuelled fire regimes aligns with findings from previous studies in TRAM (Garcia-Ruiz and Valero-Garces, 1998; Montserrat, 1992) and other Pyrenean sites such as Lourdes (Rius et al., 2011) and Marboré (Leunda et al., 2020), where such a scenario could previously only be hypothesised in the absence of robust evidence. We propose two non-exclusive, hypothesis to explain the origin of this burning dynamics:

1) Human-induced, active fires: albeit the resolution of available proxies does not always permit clear attribution to human agency (González-Sampériz et al., 2019; Rius et al., 2011), the fire activity from 4 ka BP could have been human-made in order to gain pasture areas for livestock to graze, a common tool to maintain open Pyrenean mountain landscapes (García-Ruiz et al., 2015; García-Ruiz and Lasanta, 2018). This is coincident with the general history of human impact on landscapes across the Mediterranean, where human-driven fires signs have been found since 4-3.5 ka BP (Vannière et al., 2011).

2) 2) Naturally occurring, passive fires: fires may have naturally happened, given the fire-conductive conditions existing for most of the Late Holocene. Humans could have certainly benefitted from that natural dynamics, progressively removing trees, and keeping the landscape open.

In this context, the ongoing, despite not dominant, presence of *Quercus* sp. (**Fig. 5h**) (most likely *Quercus faginea* Lam., *Q. humilis* Mill. or *Q. pubescens* Mill.) might be partly connected to a human-sustained landscape at a regional scale, as these species are both more resilient to summer drought (Laoué et al., 2023) and present resprouting abilities after fire (Milios et al., 2017), or are just more resistant to fire when these are not too intense (Trotta et al., 2024), which makes them less fire sensitive than other deciduous taxa. Additionally, the acorns of these *Quercus* species may have been valued by herders as early as four thousand years ago, particularly in the absence of alternative foraging strategies or winter fodder sources (Inácio et al., 2024). Consequently, such trees would likely have been spared from intentional burning, thereby contributing to a form of selective landscape management. This practice aligns with the concept of *landscape fruiting*—the deliberate preservation, or active conversion, into fruit-bearing landscapes for human use—coined several decades ago by González Bernáldez (1981) and applied to current day research in landscape ecology and food security (Diyaolu and Folarin, 2024; Inácio et al., 2024; Lepofsky and Lertzman, 2008). The *Abies* case is somewhat different, as this is a fire sensitive species (Kaltenrieder et al., 2010; Schwörer et al., 2015; Tinner et al., 2013) not especially resilient to human activities, even extensive grazing. The continued local presence of *Abies* in TRAM during this period supports the idea of a probably continued, low-intensity anthropogenic impact, which never reached the survival threshold for these disturbance-sensitive communities (Cagliero et al., 2023; Schwörer et al., 2015; Tinner et al., 2013). This contrast highlights a regional patched landscape where human and climatic pressures selectively shaped tree communities in concurrent areas, but far from a common vegetation landscape to the entire subalpine belt of the southern Pyrenees.

Thus, considering Tramacastilla's last millennia vegetation and fire dynamics, the progressive temperature increase (**Fig. 5m**), the constant presence of domestic animals (Julián-Posada et al., 2025), and the expansion of anthropogenic taxa (e.g. Cerealia type and *Plantago* sp., **Fig. 5e, k**), we hypothesise the existence of a millennial time scale climate-mediated human-managed landscape. Such climate-human interaction would have started ca. 6 ka BP when domestic animals arrived at TRAM, and prompted the contraction of forest biomass through the use of fire, in order to foster open ecosystems that facilitated the pasture use by their animals. A concurrent transgressive decline in temperature helped both the origin and following sustainability of these open landscapes. This trend would have been even more acute since 4.2-4 ka BP, when more frequent, human-made forest burning, and occasional natural fires, would have favoured more open communities, and aridity pulses would have maintained those open ecosystems in time. A pertinent observation is then that the landscape around TRAM over the last four millennia would have been a mosaic of different forest patches, mainly dominated by those species that can cope with low intensity impacts, either having a post-fire strategy response as some *Quercus*, or sustaining low grazers carrying capacity.

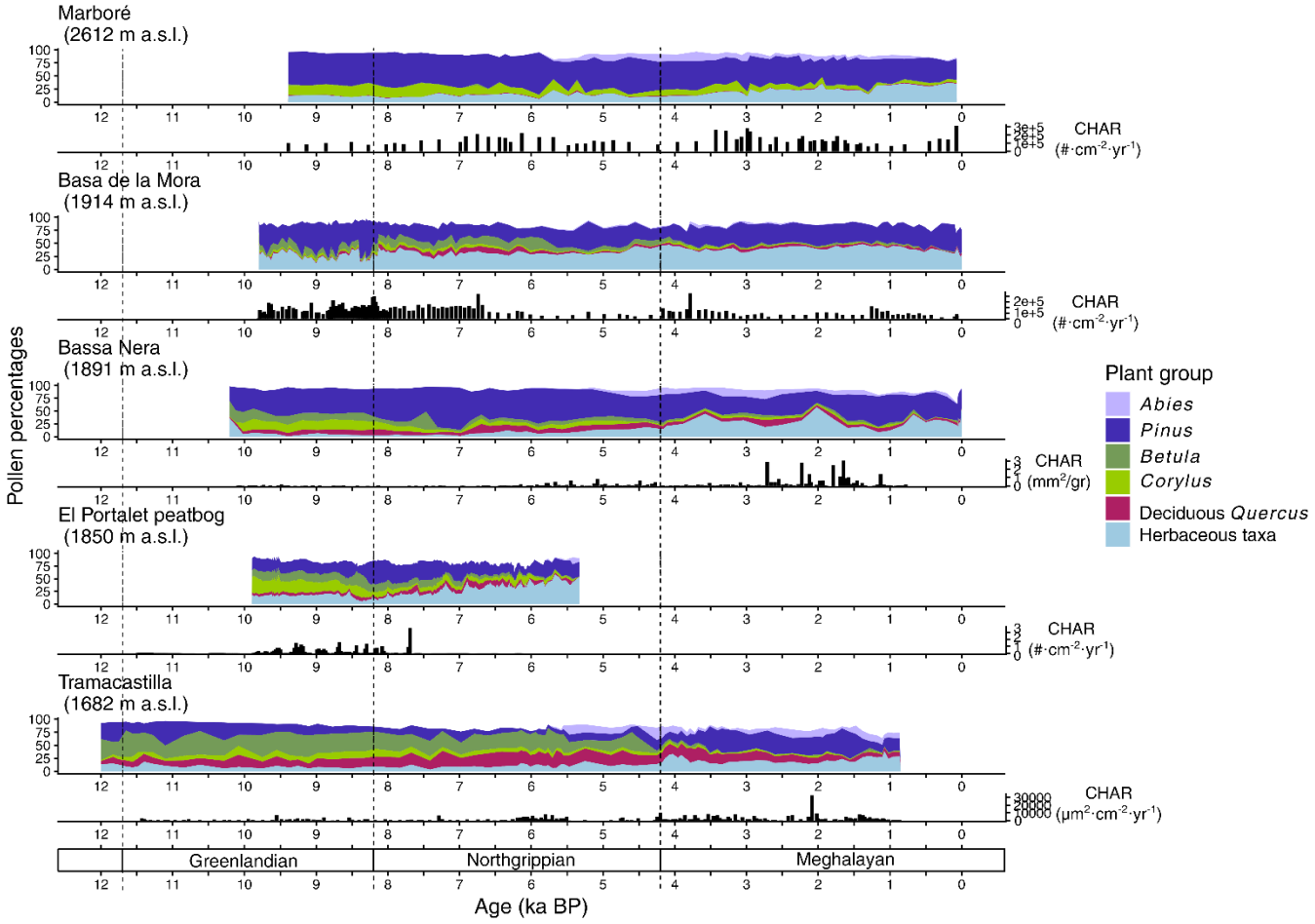


Figure 7: Synthesis of vegetation reconstructions based on pollen percentages, and fire regime reconstruction based on macrocharcoal analyses from different Pyrenean records (in altitudinal gradient): Marboré (Leunda et al., 2017, 2020), Basa de la Mora (Leunda et al., 2020; Pérez-Sanz et al., 2013), Bassa Nera (Garcés-Pastor et al., 2017), El Portalet (Gil-Romera et al., 2014; González-Sampériz et al., 2006) and Tramacastilla. Holocene subdivisions (Walker et al., 2018) are indicated at the bottom of the figure, and separated with dashed lines**.**

Contemporary and projected warming scenarios, along with the unprecedented rate of atmospheric CO_2 increase—above any levels observed over the past 800k years—and the markedly different demands of modern Western societies, complicate any direct translation of past landscapes to inform current conservation strategies in the subalpine regions of Europe. Nevertheless, the evidence presented here, together with findings from other European contexts, supports the notion of a long-standing, managed landscape in the Pyrenees extending back at least four millennia. During this time, low-intensity human interventions fostered a mosaic of patchy tree communities interspersed with pasturelands. Today, rising temperatures are accelerating woody encroachment at higher altitudes, and in the absence of integrated forest management strategies, may not only foster wildfires but prompting that these ancient open communities experience a gradual decline and, with them, the various ecosystem services they provide.

5 Conclusions

This multi-proxy study of Tramacastilla Lake provides new insights into Pyrenean landscape dynamics by combining *sed*aDNA, pollen and charcoal analysis for the last 15,000 years, being the first such integrated reconstruction in the Iberian Peninsula. It reveals complex interactions between human activities, climate and past vegetation dynamics, challenging the paradigm of early anthropogenic landscape transformation as the only factor explaining subalpine pasturelands in the Pyrenees. Our results highlight that:

- The comparison of pollen and *sed*aDNA as methodological approaches of vegetation reconstruction, while differing in some taxa, provides a more complete perspective of past vegetation dynamics.
- Landscape transformations emerged through distinct phases: initial postglacial forest expansion (14.9-11.7 ka BP) from nearby refugia also identified by *sed*aDNA; Mid-Holocene openness (6-4 ka BP) triggered by Neoglacial cooling and maintained by pastoral activities; and Late Holocene mosaic landscapes shaped by fire and grazing. Crucially, *sed*aDNA proved critical in detecting early local changes (herbaceous expansion ca. 4.5 ka BP), while charcoal revealed the shift from frequent low-intensity fires to less frequent but more intense burns after 4 ka BP.
- Climate-human interactions evolved from climate-dominated Early Holocene vegetation dynamics to synergistic drivers after 6 ka BP, when humans induced openness. This openness was possible through: 1) opportunistic exploitation by grazing (domestic animals from 6.5 ka BP); and: 2) active landscape management via selective burning and species preservation. Moreover, *sed*aDNA provided definitive evidence of anthropogenic influence through animal and plant taxa.
- Regional contextualization shows Tramacastilla's vegetation changes matched Pyrenean trends, while its disturbance regime remained partially locally distinct. This demonstrates how site-specific human practices mediated responses to regional climatic events, particularly in maintaining open mosaics during Late Holocene aridification when other areas reforested.

These results underscore the need to contextualise human activities within natural variability, as current Pyrenean landscapes represent millennia of climate-human synergy. Our study suggests that modern conservation strategies should combine ecological history with traditional practices, particularly in mountain ecosystems, where climate amplifies ecological sensitivity.

Appendix A: core correlation and chronological model

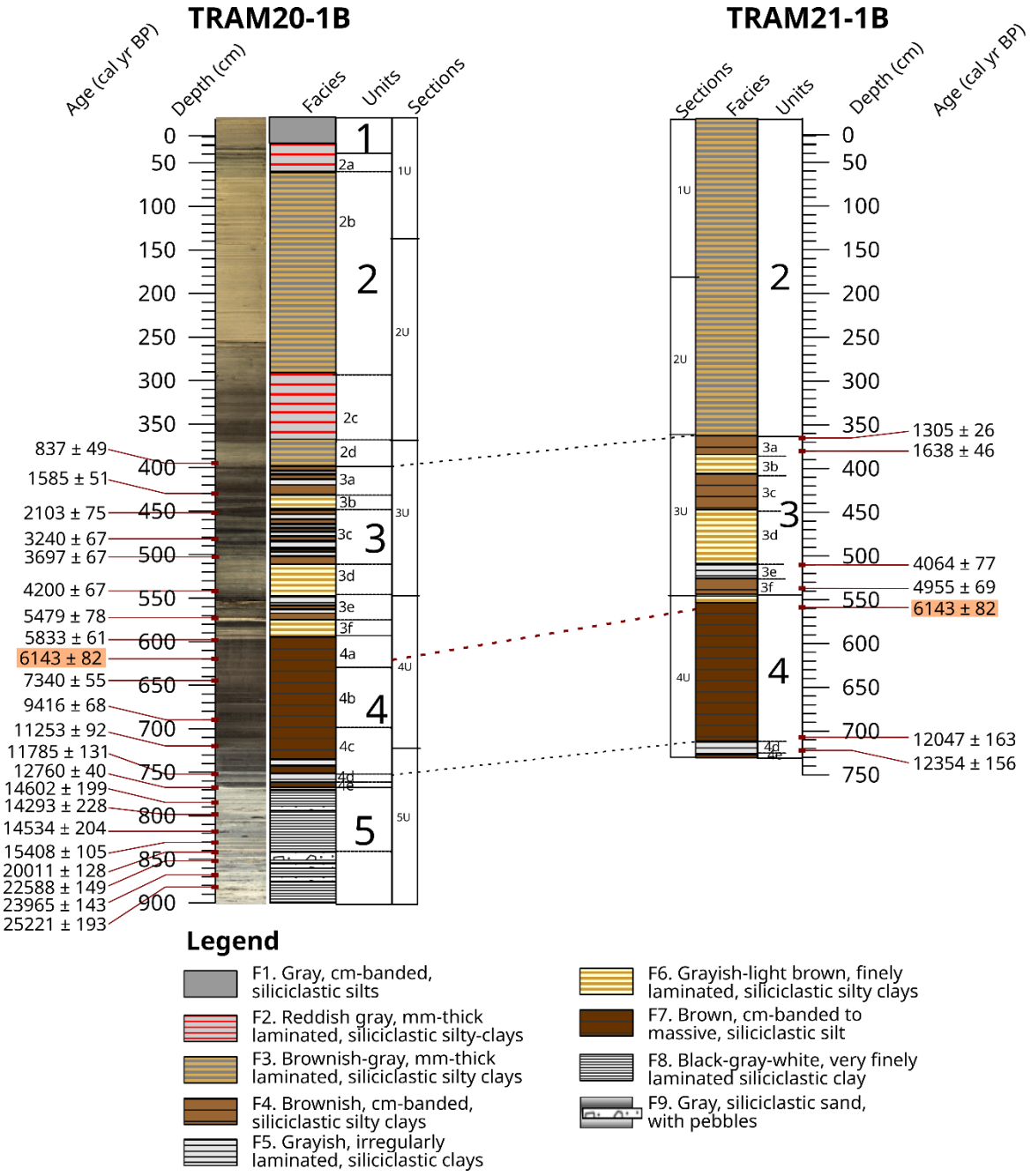
A1 Note on core correlation and chronological model

Our chronological model was created by combining radiocarbon dates from two cores (TRAM20-1B and TRAM21-1B), in order to create a complete and coherent composite sequence (**Fig. A1**). The core obtained in 2020 (TRAM20-1B) was exposed to suboptimal conditions for *sed*aDNA analyses, though it was suitable for XRF, geochemical, pollen and charcoal analyses.

The core obtained in 2021 (TRAM21-1B) was used for *sed*aDNA analyses under clean conditions. We established a chronology for core TRAM20-1B based on 21 AMS radiocarbon dates (**Table 1** and **Fig. A1**). Besides, as we dated new samples from TRAM21-1B, we integrated one of these dates into a single composite record based on the lithofacies depth correlation of both cores (**Fig. A1**). We performed such correlation using the facies description of both sequences, characterised by sediment composition, sedimentary structures and mineral composition assessed through 30 smear slides in each core under a petrographic crossed-light microscope. Sedimentary facies and sedimentological units are easily defined and correlated in both cores thus enabling transferring the date from TRAM21-1B to TRAM20-1B.

We produced a Bayesian age depth model using rbacon R package v. 3.3.1 (Blaauw and Christen, 2011) and IntCal20 calibration curve (Reimer et al., 2020). The 'rbacon' package simultaneously calibrates the input dates using IntCal20, and constructs a Bayesian age-depth model. It employs a gamma autoregressive semi-parametric model to regulate core accumulation rates, allowing for an arbitrary number of subdivisions across the sediment. As with any Bayesian inference, there are prior parameters involved, which for sediment cores include the evolution and shape (α) of accumulation rates, influencing the smoothness of the age series. Subsequently, a self-adjusting process is initiated to construct a robust age model resilient to outliers. This involves an adaptive algorithm, specifically Markov Chain Monte Carlo (MCMC), to estimate posterior distributions. Consequently, the model inherently accounts for variability in accumulation rates across different sections of a sequence. This implies that minimal variation in accumulation rates within the deposit suggests heightened "memory" or internal dependence among sequence sections. Thus, this procedure necessitates specifying the anticipated mean accumulation rate (β) and the prior for the accumulation rate's variability or "memory." Additionally, determining the number of core sections for which the MCMC process will be reiterated is crucial. We opted for a Bayesian approach as it offers the most flexible age-depth modelling strategy in archives where sedimentation rates frequently change, multiple dating methods are employed, or both. Furthermore, in the context of lake or palaeolake sequences, the deposition rate can be expressed at each depth as a weighted average of preceding depths

All parameters and information are included in https://github.com/irenejulianposada/tramacastilla_lake_multiproxy.git



735 **Figure A1: Sedimentological description and correlation between cores.** Highlighted is the date transferred from TRAM21-1B to TRAM20-1B for building the age-depth model of the master sequence. Eleven facies were identified, with sedimentological units and subunits defined in both cores.

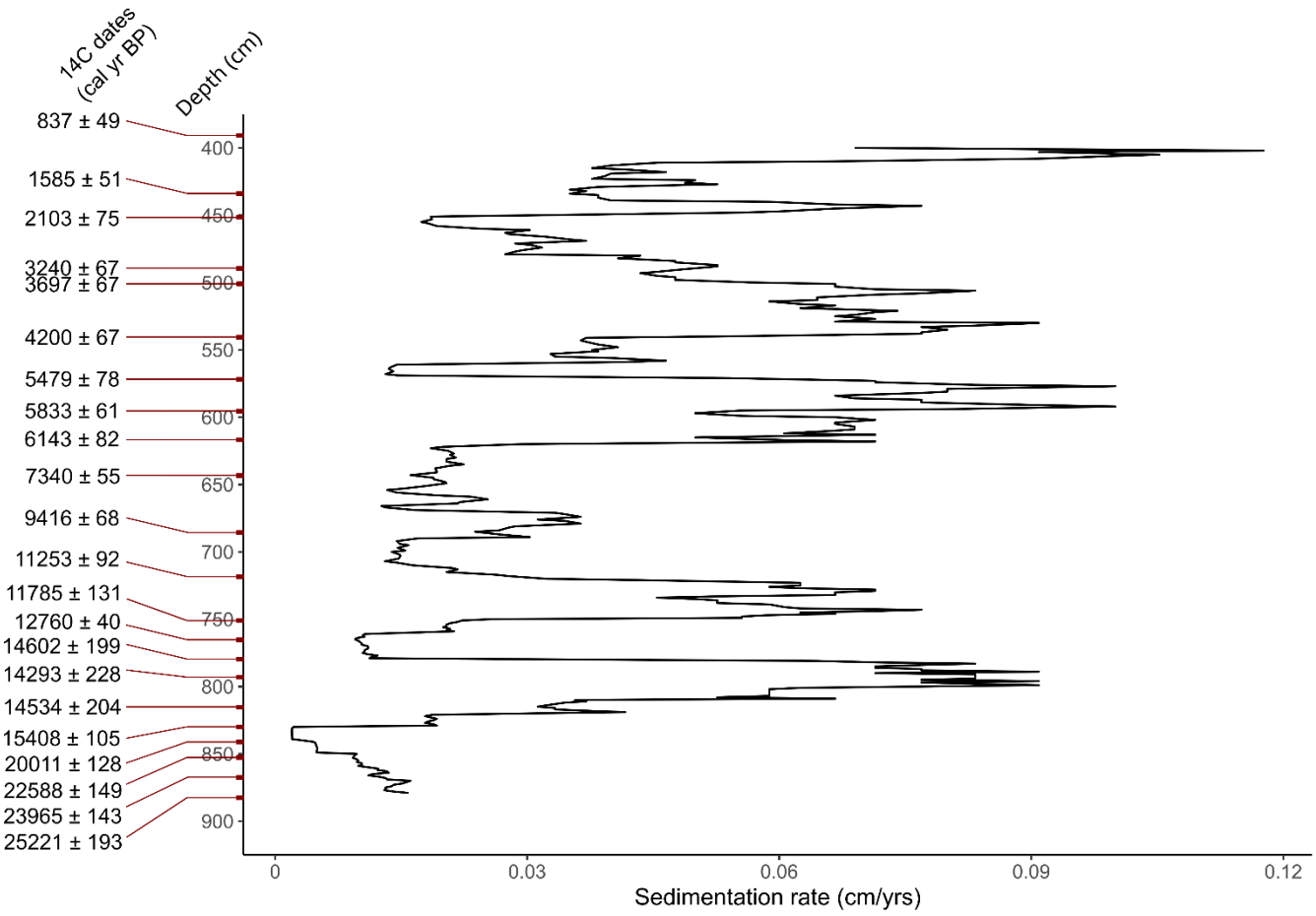


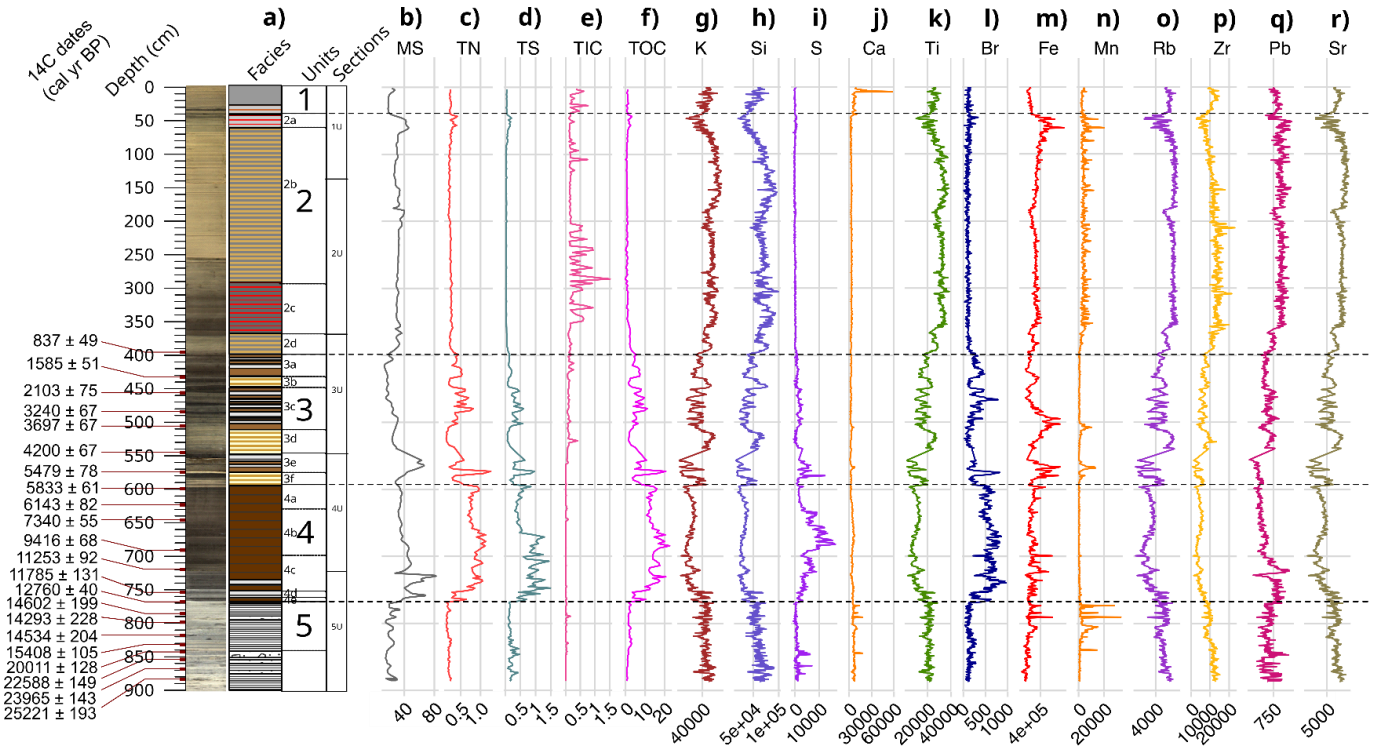
Figure A2: Changes in sedimentation rate of Tramacastilla lacustrine sequence.

Appendix B: Sedimentology and geochemistry

Table B1: Tramacastilla sedimentary facies description.

Facies ID	Sedimentological features	Geochemical composition	Depositional environment
Clastic			
F1	Gray, cm-banded, siliciclastic silts with abundant authigenic carbonate. Clay-rich matrix composed mainly of filosilicates and carbonates (rice-shaped) with silty-sized minerals, mainly quartz.	High Si and Ca, TOC ~ 0%, low Fe/Mn, low Rb/Zr	Lake with carbonate production
F2	Brownish to reddish gray, mm-thick laminated, siliciclastic silty-clays with lacustrine amorphous organic matter and rice-shaped carbonates (red laminae).	Low Si and Ca and high Fe, TOC ~ 5%, S and Br peak, high Rb/Zr	

F3 	Brownish gray, mm-thick laminated, siliciclastic silty clays. - Light laminae: low grain-size, low o.m - Dark laminae: higher grain-size, higher o.m. (terrestrial) - Intervals show red carbonate-rich laminae	High Si, Ti, and K, low Rb/Zr. Low S and TOC while TIC peaks in some intervals.	Deep lake with complete water mixing and continuous runoff events (high frequency of erosive processes)
F5 	Grayish, irregularly laminated, siliciclastic clays, slightly bioturbated (few diatoms).	High Si, K, Ti, low TOC (<5%)	Deep lake with alternation of runoff-dominated periods (F5 & F6) and in-lake productivity intervals (F4)
F6 	Grayish-light brown, finely laminated, siliciclastic silty-clays (very few diatoms)	Very high Si, K and Ti and very low S, TOC (< 2%) and Br	
F8 	Black-gray-white, very finely laminated siliciclastic clays.	Very high Si, K and Ti, low S, TOC (~ 3%) and low Br. High Rb/Zr	Sedimentation dominated by runoff and clay decantation (frozen lake?) processes in a very cold/dry environment
F9 	Grayish, mm-thick irregular lamination, siliciclastic fine silts. Alternation with coarser layers, sometimes with pebbles (limestones?).	Very high Si, K and Ti, low S, TOC (~ 0%) and low Br	Sedimentation dominated by runoff processes in a glacial environment (dropstones)
Organic-rich			
F4 	Brownish, cm-banded, siliciclastic silty clays with lacustrine amorphous organic matter and diatoms	Low Si, K, Ti, TOC ~ 5%, High S and Br	Deep lake with alternation of runoff-dominated periods (F5 & F6) and in-lake productivity intervals (F4)
F7 	Dark brown, cm-banded to massive, siliciclastic silty-clays with high organic matter (no diatoms)	Low Si, K, Ti, TOC > 10%, high S and Br and high Fe/Mn variability. Presence of vivianite.	Highly productive lake (eutrophic), with episodic anoxia in the bottom waters (no mixing continuously)



745 **Figure B1: Mineralogical and geochemical measurements for Tramacastilla:** a) high-resolution photo, sedimentary facies, units and subunits; b) MS-magnetic susceptibility (SI x 10^{-5}); c-f) LECO analysis in %, including TN-Total Nitrogen, TS-Total Sulphur, TIC-Total Inorganic Carbon, TOC-Total Organic Carbon; and g-r) selection of X-Ray Fluorescence data (K, Si, S, Ca, Ti, Br, Fe, Mn, Rb, Zr, Pb, Sr, measured in counts per second).

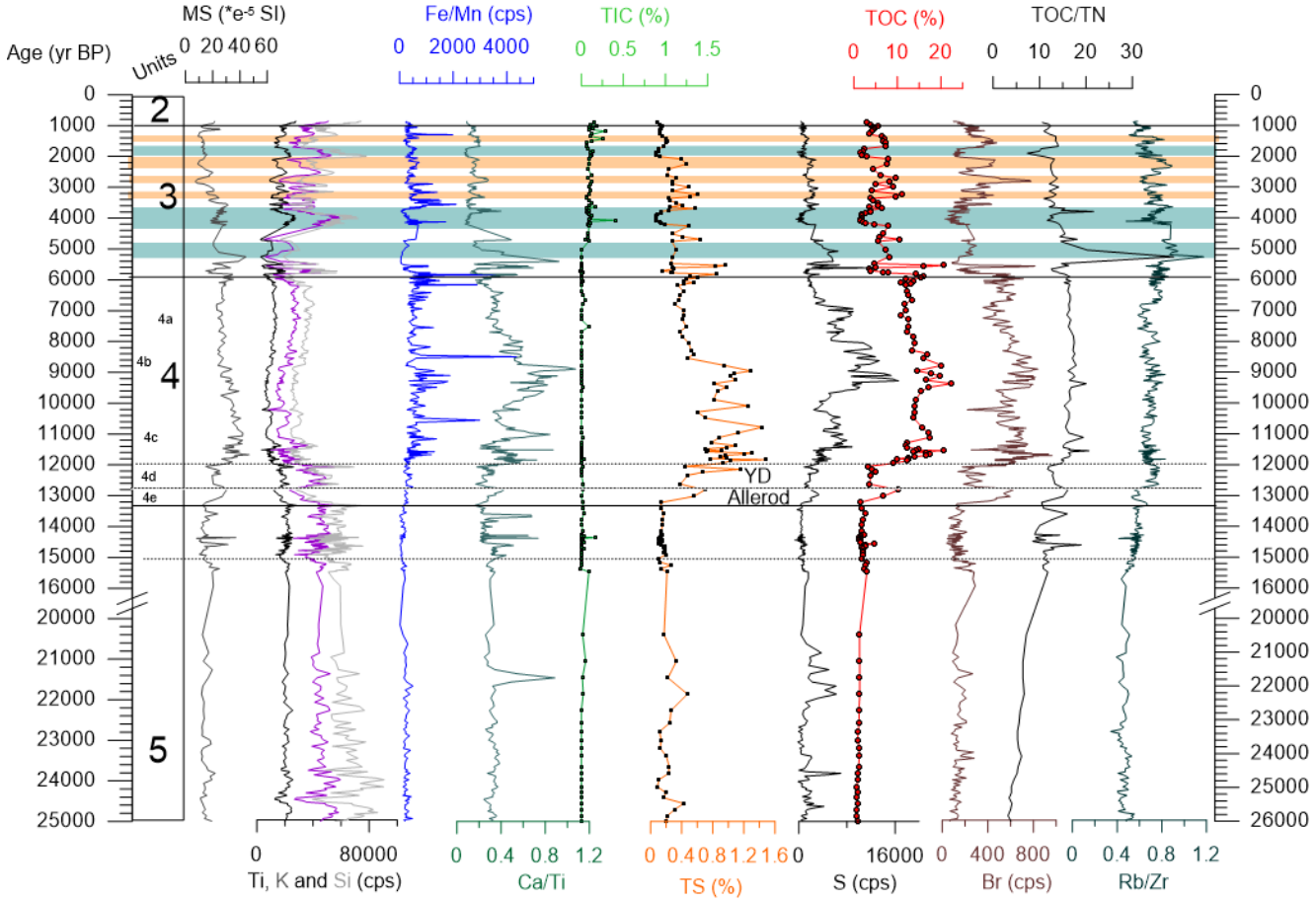


Figure B2: Synthesis of mineralogical and geochemical results for Tramacastilla sequence represented against age (ka BP). Includes: sedimentary units and subunits; MS - magnetic susceptibility (SI x 10^{-5}); selection of X-Ray fluorescence data (Ti, K, Si, Fe/Mn, Ca/Ti, S, Br, Rb/Zr, measured in counts per second); TIC - total inorganic Carbon (%); TS - total Sulphur (%); TOC - total organic Carbon (%) and TOC/TN.

Appendix C: Biological analyses

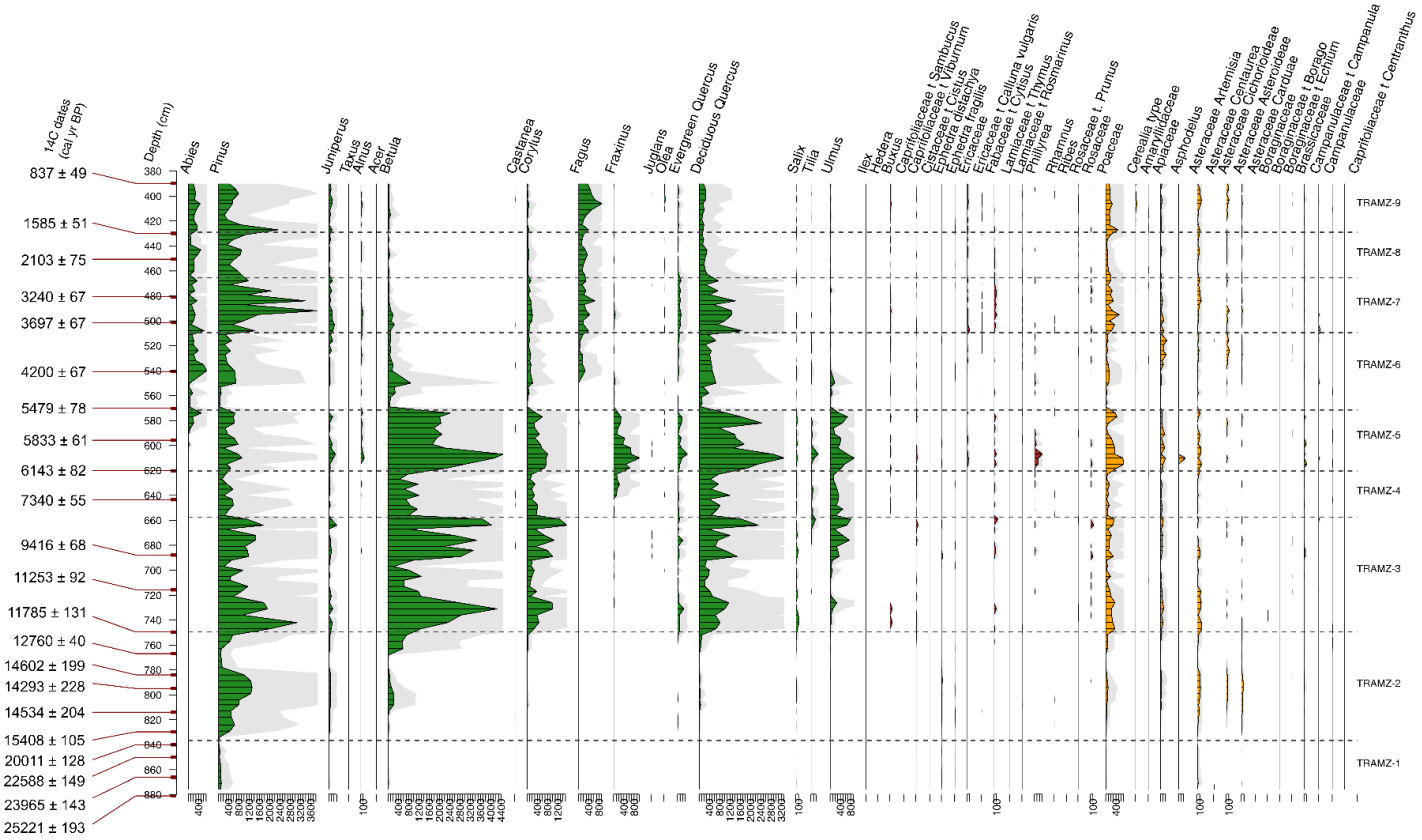


Figure C1: Pollen percentages of all pollen types that occur throughout the Tramacastilla record, with CONISS zones (TRAMZ-1 to 9) indicated in the right side. Green is used for trees, dark red for shrubs and orange for herbs pollen types.

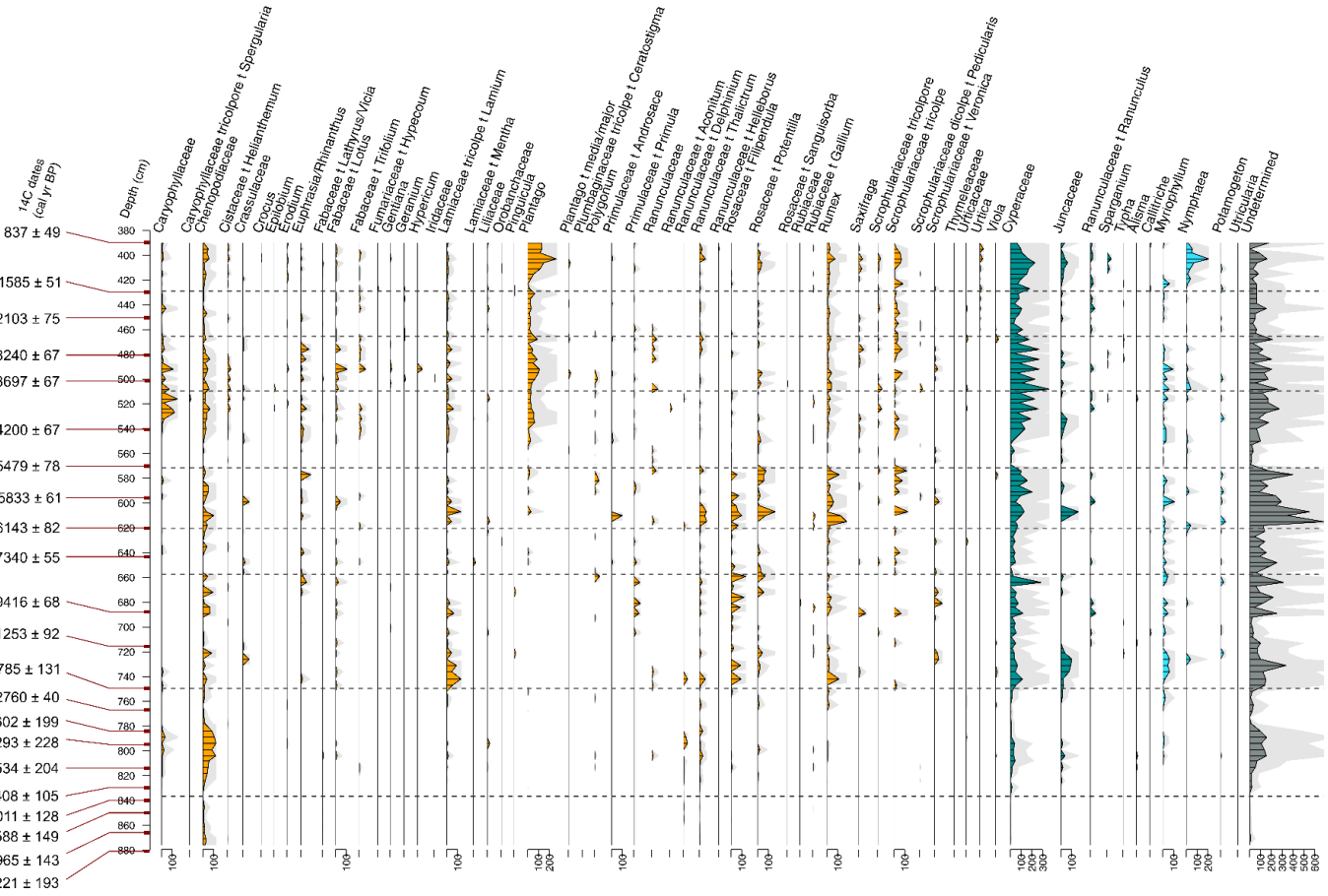
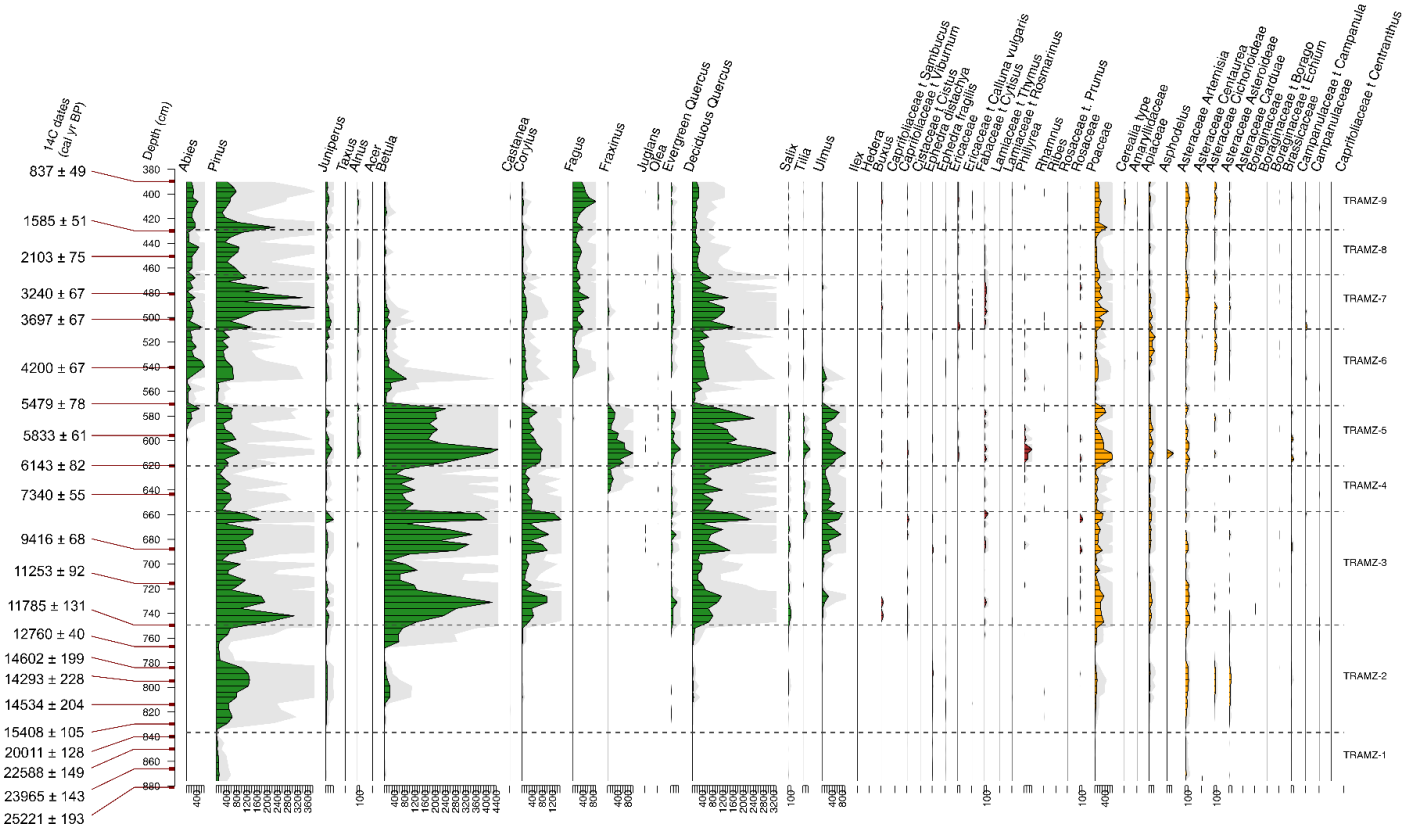


Figure C2: Pollen percentages of all pollen types that occur throughout the Tramacastilla record, with CONISS zones (TRAMZ-1 to 9) indicated in the right side. Orange is used for herbs, dark blue for hygrophytes, light blue for hydrophytes and grey for undetermined pollen types.



765 **Figure C3: PAR values of all pollen types that occur throughout the Tramacastilla record, with CONISS zones (TRAMZ-1 to 9) indicated in the right side.** Green is used for trees, dark red for shrubs and orange for herbs pollen types.

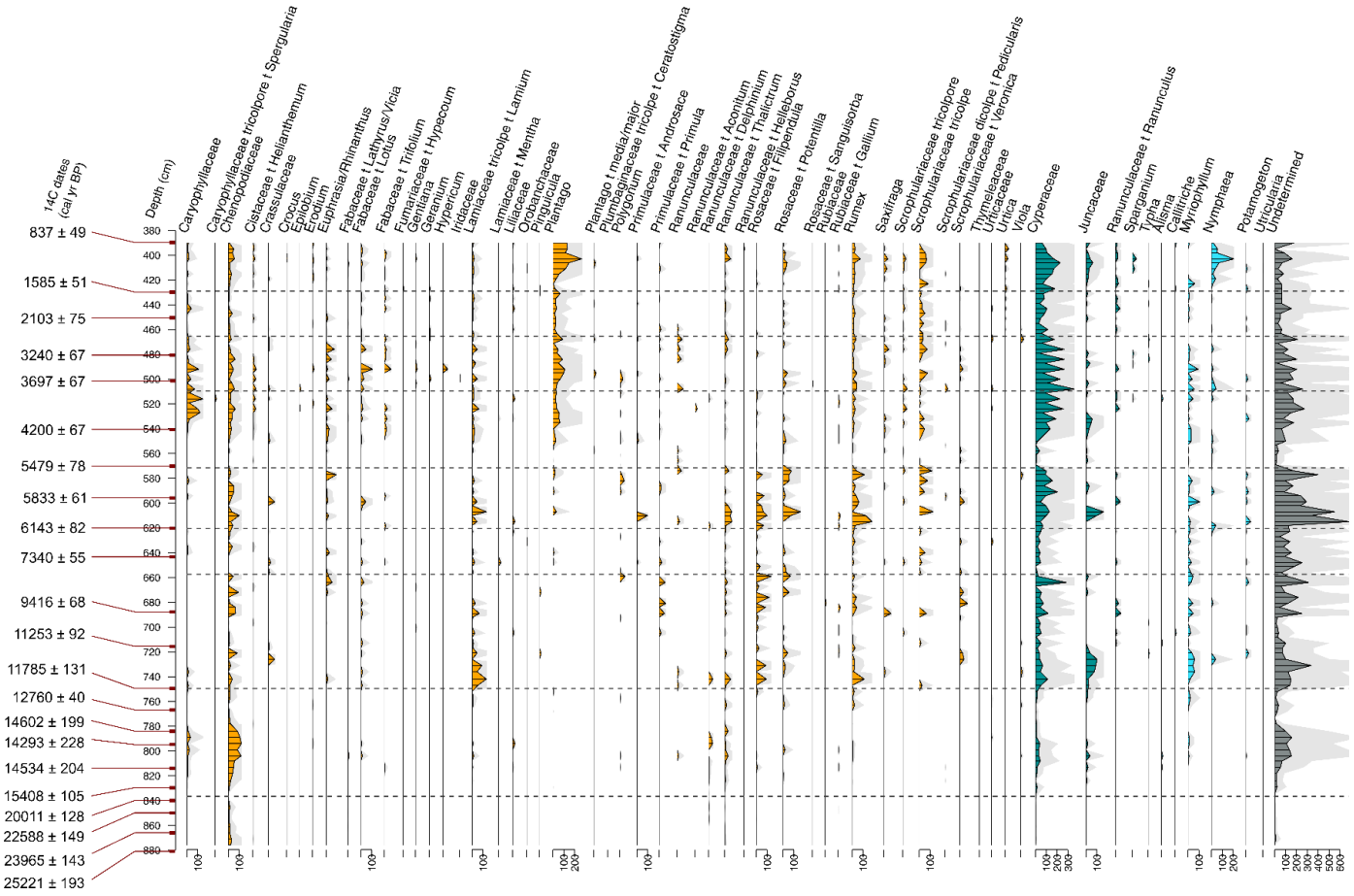


Figure C4: . PAR values of all pollen types that occur throughout the Tramacastilla record, with CONISS zones (TRAMZ-1 to 9) indicated in the right side. Orange is used for herbs, dark blue for hygrophytes, light blue for hydrophytes and grey for undetermined pollen types.

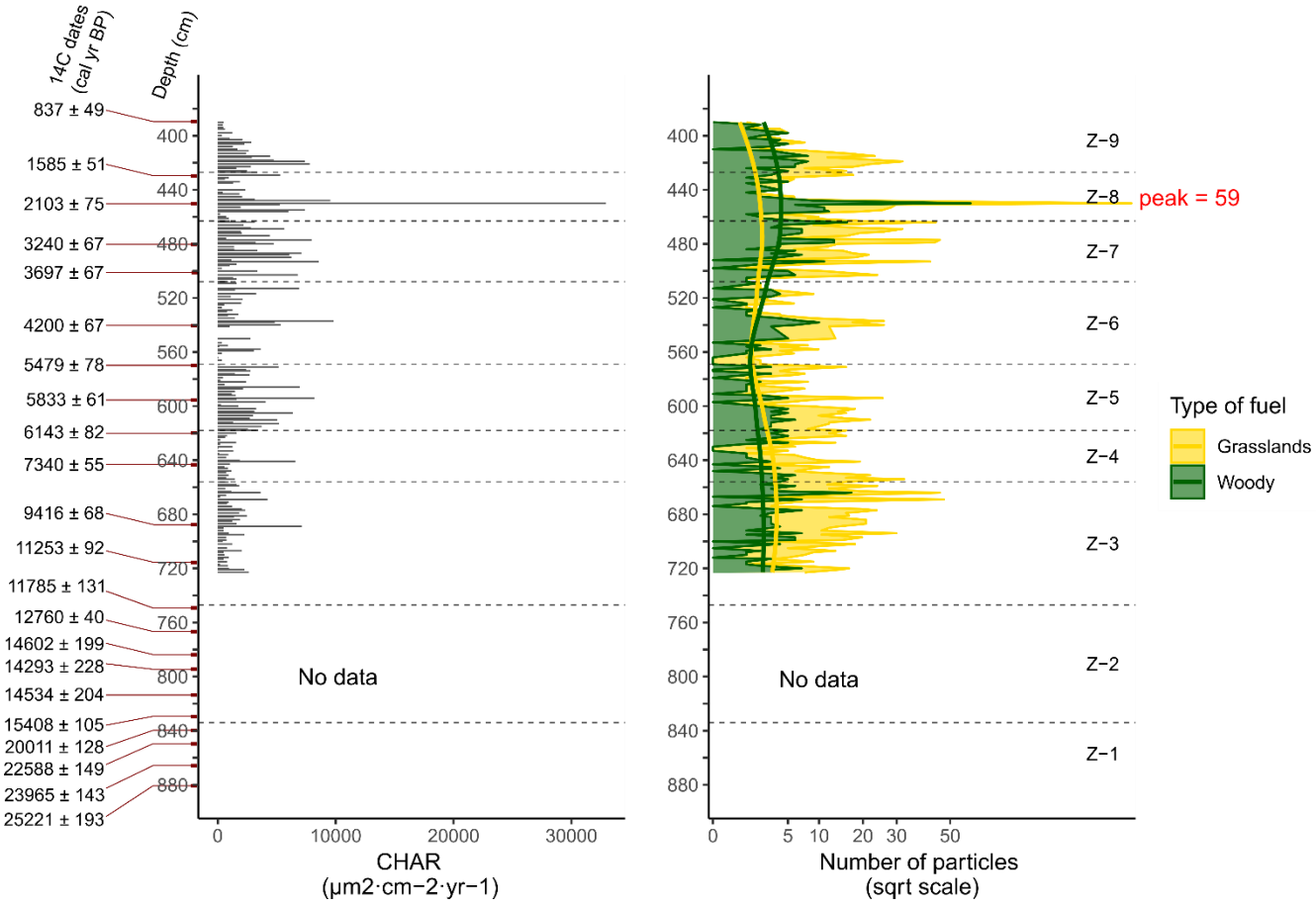


Figure C5: Charcoal results synthesis, including CHAR influx (µm²·cm⁻²·yr⁻¹) and width to length (W/L) ratio. Yellow and green silhouettes represent the total number of particles in each sediment sample with a width-to-length (W/L) ratio < 0.5 (indicative of herbaceous fuel) and > 0.5 (indicative of woody fuel), respectively. Smoothed lines highlight the predominant fuel type: yellow for herbaceous and green for woody vegetation. Separated with dashed lines are CONISS-made pollen zones (TRAMZ-1 to 9).

Table C1: Summary of biological analyses results.

Proxy	Measurement	Min	Max	Mean	SD
Pollen analysis	Terrestrial pollen grains per sample	313	604	425.7	58.9
	Terrestrial pollen types per sample	13	47	27	7.9
	Terrestrial PAR (number of grains·cm^{-2}·yr^{-1})	27.4	13867.5	3399.8	2942.8
Charcoal analysis	Charcoal particles per sample	0	83	6.33	7.35
	Charcoal area per sample (mm^2)	0	4.23	0.23	0.37
	Width to length (W/L) ratio	0.05	1	0.55	0.26
	CHAR (µm^2·cm^{-2}·yr^{-1})	0	32926.8	2298.2	3017.6

Code and data availability.

The numerical workflow of this study is stored in Github (https://github.com/irenejulianposada/tramacastilla_lake_multiproxy.git), and the processed data and supplementary data in Zenodo (10.5281/zenodo.19917887).

Author contributions

Conceptualization: PGS, AM, GGR; Funding acquisition: PGS, AM; Field expedition coordination: GGR; Fieldwork campaigns: IJP, GGR, AM, BVG, PGS; Age-depth model and sedimentological analyses: IJP, GGR, AM, BVG; Pollen and charcoal counting: IJP; Charcoal analyses supervision: GGR, BL; Data curation and visualisation: IJP; Writing – original draft: IJP; Writing – review and editing: GGR, BL, AM, BVG, PGS.

Competing interests

The authors declare that they have no conflict of interest.

Acknowledgements

Funding for this research was provided by the Spanish Ministry of Science and Innovation through the PYCACHU project (PID2019-106050RB-I00), CORREDORAS project (PID2022-141558NB-I00) and PASTORA project (OAPN, ref. 2852/2022), as well as the E02_23R research group of Gobierno de Aragón. Irene Julián Posada was supported by a PhD fellowship provided by the Spanish Ministry of Science, Innovation and Universities (FPI PRE2020 094749). The authors wish to acknowledge Scientific and Technique Analysis Services in Pyrenean Institute of Ecology-CSIC in Zaragoza-Jaca (Spain) for their technical and analytical support, especially Elena Royo, Pilar Eseverri, Inés de la Parra and Daniel Sánchez for the laboratory work. We are grateful to the Gobierno de Aragón and the Tramacastilla de Tena town council for granting the permissions needed for the sampling process. We thank Miguel Bartolomé, Marcel Galofré, Javier Lara-Recuero, Kilian Jungkeit-Milla, Reyes Giménez, Benito Pérez, Jorge Pey, Pedro Sánchez for their help in the field campaigns.

References

Alday, A., Domingo, R., Sebastián, M., Soto, A., Aranbarri, J., González-Sampériz, P., Sampietro-Vattuone, M. M., Utrilla, P., Montes, L., and Peña-Monné, J. L.: The silence of the layers: Archaeological site visibility in the Pleistocene-Holocene transition at the Ebro Basin, Quaternary Science Reviews, 184, 85–106, https://doi.org/10.1016/j.quascirev.2017.11.006, 2018.

Ali, A. A., Higuera, P. E., Bergeron, Y., and Carcaillet, C.: Comparing fire-history interpretations based on area, number and estimated volume of macroscopic charcoal in lake sediments, Quaternary Research, 72, 462–468, https://doi.org/10.1016/j.yqres.2009.07.002, 2009.

Alsos, I. G., Sjögren, P., Edwards, M. E., Landvik, J. Y., Gielly, L., Forwick, M., Coissac, E., Brown, A. G., Jakobsen, L. V., Føreid, M. K., and Pedersen, M. W.: Sedimentary ancient DNA from Lake Skartjørna, Svalbard: Assessing the resilience of arctic flora to Holocene climate change, The Holocene, 26, 627–642, https://doi.org/10.1177/0959683615612563, 2016.

Alsos, I. G., Lammers, Y., Yoccoz, N. G., Jørgensen, T., Sjögren, P., Gielly, L., and Edwards, M. E.: Plant DNA metabarcoding of lake sediments: How does it represent the contemporary vegetation, PLoS ONE, 13, e0195403, https://doi.org/10.1371/journal.pone.0195403, 2018.

Araus, J. l., Febrero, A., Buxo, R., Camalich, M. d., Martin, D., Molina, F., Rodriguez-Ariza, M. o., and Romagosa, I.: Changes in carbon isotope discrimination in grain cereals from different regions of the western Mediterranean Basin during the past seven millennia. Palaeoenvironmental evidence of a differential change in aridity during the late Holocene, Global Change Biology, 3, 107–118, https://doi.org/10.1046/j.1365-2486.1997.00056.x, 1997.

Archibald, S., Lehmann, C. E. R., Gómez-Dans, J. L., and Bradstock, R. A.: Defining pyromes and global syndromes of fire regimes, Proc. Natl. Acad. Sci. U.S.A., 110, 6442–6447, https://doi.org/10.1073/pnas.1211466110, 2013.

Aregger, S. C., Van Vugt, L., Gobet, E., Zahajská, P., Nielsen, E. H., Boschetti, A., Hafner, A., Schwörer, C., Vogel, H., Erb, M., Erb, U., and Tinner, W.: Climate and human forcing of montane vegetation dynamics during the past 15,600 years in the Simmental, Northern Swiss Alps, Quaternary Science Reviews, 366, 109470, https://doi.org/10.1016/j.quascirev.2025.109470, 2025.

Aurelle, D., Thomas, S., Albert, C., Bally, M., Bondeau, A., Boudouresque, C., Cahill, A. E., Carlotti, F., Chenuil, A., Cramer, W., Davi, H., De Jode, A., Ereskovsky, A., Farnet, A., Fernandez, C., Gauquelin, T., Mirleau, P., Monnet, A., Prévosto, B., Rossi, V., Sartoretto, S., Van Wambeke, F., and Fady, B.: Biodiversity, climate change, and adaptation in the Mediterranean, Ecosphere, 13, e3915, https://doi.org/10.1002/ecs2.3915, 2022.

Ausín, B., García-Alix, A., Hernández, A., González-Rouco, J. F., Montoya, M., Cacho, I., Moreno Caballud, A., Abel Schaad, D., Alba Sánchez, F., Bao, R., Benito, X., Camuera, J., Vara, A. de la, Domínguez-Castro, F., Domínguez-Villar, D., Dorado-Liñán, I., García-Pereira, F., Gázquez Sánchez, F., Gómez-Navarro, J. J., González-Sampériz, P., Jiménez de Cisneros, C., Jiménez-Espejo, F. J., Jiménez-Moreno, G., Lakrani, P., Lebreiro, S., López-Blanco, C., López Sáez, J. A., Martín-Chivelet, J., Martínez-Ruíz, F. C., Martrat, B., Morellón, M., Pelejero, C., Tarruella, J. P., Pontevedra Pombal, X., Rodrigo Gámiz, M., Rodrigues, T., Rodrigo, F. S., Sierro, F. J., Tejedor, E., Vaquero, J. M., and Voelker, A. H. L.: Atmospheric and Oceanic Changes Since the Last Glacial Maximun: Review of Proxy-Based and Climate Model Simulation Reconstructions in the Iberian Península, in: The CLIVAR-Spain report on the climate in Spain, Ministerio para la Transición Ecológica y el Reto Demográfico (España), 18–82, https://doi.org/10.13039/501100000780, 2024.

Bartolomé, M., Moreno, A., Sancho, C., Stoll, H. M., Cacho, I., Spötl, C., Belmonte, Á., Edwards, R. L., Cheng, H., and Hellstrom, J. C.: Hydrological change in Southern Europe responding to increasing North Atlantic overturning during Greenland Stadial 1, Proc. Natl. Acad. Sci. U.S.A., 112, 6568–6572, https://doi.org/10.1073/pnas.1503990112, 2015.

Bernal-Wormull, J. L., Moreno, A., Bartolomé, M., Arriolabengoa, M., Pérez-Mejías, C., Iriarte, E., Osácar, C., Spötl, C., Stoll, H., Cacho, I., Edwards, R. L., and Cheng, H.: New insights into the climate of northern Iberia during the Younger Dryas and Holocene: The Mendukilo multi-speleothem record, Quaternary Science Reviews, 305, 108006, https://doi.org/10.1016/j.quascirev.2023.108006, 2023.

Blaauw, M. and Christen, J. A.: Flexible paleoclimate age-depth models using an autoregressive gamma process, Bayesian Analysis, 6, 457–474, https://doi.org/10.1214/11-BA618, 2011.

Cacho, I., Grimalt, J. O., Canals, M., Sbaffi, L., Shackleton, N. J., Schönfeld, J., and Zahn, R.: Variability of the western Mediterranean Sea surface temperature during the last 25,000 years and its connection with the Northern Hemisphere climatic changes, Paleoceanography, 16, 40–52, https://doi.org/10.1029/2000PA000502, 2001.

Cagliero, E., Paradis, L., Marchi, N., Lisztes-Szabó, Z., Braun, M., Hubay, K., Sabatier, P., Čurović, M., Spalevic, V., Motta, R., Lingua, E., and Finsinger, W.: The role of fire disturbances, human activities and climate change for long-term forest dynamics in upper-montane forests of the central Dinaric Alps, The Holocene, 33, 827–841, https://doi.org/10.1177/09596836231163515, 2023.

Carrión, J. S., Fernández, S., González-Sampériz, P., Gil-Romera, G., Badal, E., Carrión-Marco, Y., López-Merino, L., López-Sáez, J. A., Fierro, E., and Burjachs, F.: Expected trends and surprises in the Lateglacial and Holocene vegetation history of the Iberian Peninsula and Balearic Islands, Review of Palaeobotany and Palynology, 162, 458–475, https://doi.org/10.1016/j.revpalbo.2009.12.007, 2010.

Casas, D. G. and Gassiot-Ballbè, E.: The Archaeology of Pastoralism in the Central Pyrenees: A Diachronic Analysis of Livestock Structures in Aigüestortes i Estany de Sant Maurici National Park, Journal of Mediterranean Archaeology, 5–31, 2022.

Connor, S. E., Vannière, B., Colombaroli, D., Anderson, R. S., Carrión, J. S., Ejarque, A., Gil Romera, G., González-Sampériz, P., Hoefer, D., Morales-Molino, C., Revelles, J., Schneider, H., Van Der Knaap, W. O., Van Leeuwen, J. F., and Woodbridge, J.: Humans take control of fire-driven diversity changes in Mediterranean Iberia's vegetation during the mid–late Holocene, The Holocene, 29, 886–901, https://doi.org/10.1177/0959683619826652, 2019.

Costa, M., Morla, C., and Sainz, H.: Los bosques ibéricos: una interpretación geobotánica, 4. ed., Planeta, Barcelona, 597 pp., 2005.

Cunill, R., Soriano, J. M., Bal, M. C., Pèlachs, A., Rodriguez, J. M., and Pérez-Obiol, R.: Holocene high-altitude vegetation dynamics in the Pyrenees: A pedoanthracology contribution to an interdisciplinary approach, Quaternary International, 289, 60–70, https://doi.org/10.1016/j.quaint.2012.04.041, 2013.

Currás, A., Zamora, L., Reed, J. M., García-Soto, E., Ferrero, S., Armengol, X., Mezquita-Joanes, F., Marqués, M. A., Riera, S., and Julià, R.: Climate change and human impact in central Spain during Roman times: High-resolution multi-proxy analysis of a tufa lake record (Somolinos, 1280 m asl), CATENA, 89, 31–53, https://doi.org/10.1016/j.catena.2011.09.009, 2012.

Daniau, A.-L., Sánchez-Goñi, M. F., Beaufort, L., Laggoun-Défarge, F., Loutre, M.-F., and Duprat, J.: Dansgaard–Oeschger climatic variability revealed by fire emissions in southwestern Iberia, Quaternary Science Reviews, 26, 1369–1383, https://doi.org/10.1016/j.quascirev.2007.02.005, 2007.

Deza-Araujo, M., Morales-Molino, C., Tinner, W., Henne, P. D., Heitz, C., Pezzatti, G. B., Hafner, A., and Conedera, M.: A critical assessment of human-impact indices based on anthropogenic pollen indicators, Quaternary Science Reviews, 236, 106291, https://doi.org/10.1016/j.quascirev.2020.106291, 2020.

Deza-Araujo, M., Morales-Molino, C., Conedera, M., Pezzatti, G. B., Pasta, S., and Tinner, W.: Influence of taxonomic resolution on the value of anthropogenic pollen indicators, Veget Hist Archaeobot, 31, 67–84, https://doi.org/10.1007/s00334-021-00838-x, 2022.

Di Rita, F., Fletcher, W. J., Aranbarri, J., Margaritelli, G., Lirer, F., and Magri, D.: Holocene forest dynamics in central and western Mediterranean: periodicity, spatio-temporal patterns and climate influence, Sci Rep, 8, 8929, https://doi.org/10.1038/s41598-018-27056-2, 2018.

Dietre, B., Reitmaier, T., Walser, C., Warnk, T., Unkel, I., Hajdas, I., Lambers, K., Reidl, D., and Haas, J. N.: Steady transformation of primeval forest into subalpine pasture during the Late Neolithic to Early Bronze Age (2300−1700 BC) in the Silvretta Alps, Switzerland, The Holocene, 30, 355–368, https://doi.org/10.1177/0959683619887419, 2020.

Diyaolu, C. O. and Folarin, I. O.: The Role of Biodiversity in Agricultural Resilience: Protecting Ecosystem Services for Sustainable Food Production, Int. J. Res. Publ. Rev., 5, 1560–1573, https://doi.org/10.55248/gengpi.5.1024.2741, 2024.

Dziomber, I., Gobet, E., Leunda, M., Gurtner, L., Vogel, H., Tournier, N., Damanik, A., Szidat, S., Tinner, W., and Schwörer, C.: Palaeoecological multiproxy reconstruction captures long-term climatic and anthropogenic impacts on vegetation dynamics in the Rhaetian Alps, Review of Palaeobotany and Palynology, 321, 105020, https://doi.org/10.1016/j.revpalbo.2023.105020, 2024.

Ejarque, A., Julià, R., Riera, S., Palet, J. M., Orengo, H. A., Miras, Y., and Gascón, C.: Tracing the history of highland human management in the eastern Pre-Pyrenees: an interdisciplinary palaeoenvironmental study at the Pradell fen, Spain, The Holocene, 19, 1241–1255, https://doi.org/10.1177/0959683609345084, 2009.

Ejarque, A., Miras, Y., Riera, S., Palet, J. M., and Orengo, H. A.: Testing micro-regional variability in the Holocene shaping of high mountain cultural landscapes: a palaeoenvironmental case-study in the eastern Pyrenees, Journal of Archaeological Science, 37, 1468–1479, https://doi.org/10.1016/j.jas.2010.01.007, 2010.

Ellis, E. C.: Land Use and Ecological Change: A 12,000-Year History, Annu. Rev. Environ. Resour., 46, 1–33, https://doi.org/10.1146/annurev-environ-012220-010822, 2021.

Fabre, M., Forest, V., Ranché, C., Fiorillo, D., Casabianca, F., Vigne, J.-D., and Balasse, M.: Milk and meat exploitation, autumn lambing and use of forest resources in Neolithic Corsican sheep farming systems (fifth to third millennia cal BC), Journal of Archaeological Science: Reports, 50, 104037, https://doi.org/10.1016/j.jasrep.2023.104037, 2023.

Felde, V. A., Mottl, O., Flantua, S. G. A., Bhatta, K. P., Birks, H. H., Grytnes, J.-A., Hooghiemstra, H., Nogué, S., Reitalu, T., Seddon, A. W. R., Steinbauer, M. J., Braak, C. J. F. T., Giesecke, T., Goring, S. J., Haberle, S. G., Herbert, A. V., Šmilauer, P., Tinner, W., Williams, J. W., Bird, D., Freeman, J., Gayo, E., Hoggarth, J. A., Latorre, C., Miranda, L., Robinson, E., Cao, X., Chen, F., and Birks, H. J. B.: Climate outweighs human effects on vegetation properties during the early-to-mid Holocene, https://doi.org/10.21203/rs.3.rs-4692574/v1, 10 July 2024., 2024.

Finsinger, W. and Iago-Lito: tapas: an R package to perform trend and peaks analysis (v0.1.0), https://doi.org/10.5281/ZENODO.6344463, 2022.

Finsinger, W., Kelly, R., Fevre, J., and Magyari, E. K.: A guide to screening charcoal peaks in macrocharcoal-area records for fire-episode reconstructions, The Holocene, 24, 1002–1008, https://doi.org/10.1177/0959683614534737, 2014.

Galop, D.: Estives d'Ossau: 7000 ans de pastoralisme dans les Pyrénées, le Pas d'oiseau FRAMESPA Parc national des Pyrénées, Toulouse Tarbes, 2016.

Garcés-Pastor, S., Cañellas-Boltà, N., Pèlachs, A., Soriano, J.-M., Pérez-Obiol, R., Pérez-Haase, A., Calero, M.-A., Andreu, O., Escolà, N., and Vegas-Vilarrúbia, T.: Environmental history and vegetation dynamics in response to climate variations and human pressure during the Holocene in Bassa Nera, Central Pyrenees, Palaeogeography, Palaeoclimatology, Palaeoecology, 479, 48–60, https://doi.org/10.1016/j.palaeo.2017.04.016, 2017.

Garcés-Pastor, S., Coissac, E., Lavergne, S., Schwörer, C., Theurillat, J.-P., Heintzman, P. D., Wangensteen, O. S., Tinner, W., Rey, F., Heer, M., Rutzer, A., Walsh, K., Lammers, Y., Brown, A. G., Goslar, T., Rijal, D. P., Karger, D. N., Pellissier, L., The PhyloAlps Consortium, Heiri, O., and Alsos, I. G.: High resolution ancient sedimentary DNA shows that alpine plant diversity is associated with human land use and climate change, Nat Commun, 13, 6559, https://doi.org/10.1038/s41467-022-34010-4, 2022.

García, M. B., Miranda, H., Pizarro, M., Font, X., Roquet, C., and González-Sampériz, P.: Habitats hold an evolutionary signal of past climatic refugia, Biodivers Conserv, 31, 1665–1688, https://doi.org/10.1007/s10531-022-02419-4, 2022.

García-Ruiz, J. M. and Lasanta, T.: El Pirineo Aragonés como paisaje cultural, Pirineos, 173, e038, https://doi.org/10.3989/pirineos.2018.173005, 2018.

Garcia-Ruiz, J. M. and Valero-Garces, B. L.: Historical Geomorphic Processes and Human Activities in the Central Spanish Pyrenees, Mountain Research and Development, 18, 309, https://doi.org/10.2307/3674096, 1998.

García-Ruiz, J. M., Martí-Bono, C., Valero-Garcés, B. L., and González-Sampériz, P.: La evolución de los glaciares del Pleistoceno Superior en el Pirineo Central español. El ejemplo de los glaciares de Escarra y Lana Mayor, Alto Valle del Gállego, Rev. C. y G., 15, 103–119, 2001.

García-Ruiz, J. M., López-Moreno, J. I., Lasanta, T., Vicente-Serrano, S. M., González-Sampériz, P., Valero-Garcés, B. L., Sanjuán, Y., Beguería, S., Nadal-Romero, E., Lana-Renault, N., and Gómez-Villar, A.: Los efectos geoecológicos del cambio global en el Pirineo Central español: una revisión a distintas escalas espaciales y temporales, Pirineos, 170, e012, https://doi.org/10.3989/Pirineos.2015.170005, 2015.

García-Ruiz, J. M., Palacios, D., Andrés, N., and López-Moreno, J. I.: Neoglaciation in the Spanish Pyrenees: a multiproxy challenge, Med. Geosc. Rev., 2, 21–36, https://doi.org/10.1007/s42990-020-00022-9, 2020a.

García-Ruiz, J. M., Tomás-Faci, G., Diarte-Blasco, P., Montes, L., Domingo, R., Sebastián, M., Lasanta, T., González-Sampériz, P., López-Moreno, J. I., Arnáez, J., and Beguería, S.: Transhumance and long-term deforestation in the subalpine belt of the central Spanish Pyrenees: An interdisciplinary approach, CATENA, 195, 104744, https://doi.org/10.1016/j.catena.2020.104744, 2020b.

Gassiot-Ballbè, E., Mazzucco, N., Clemente-Conte, I., Rodríguez Antón, D., Obea-Gómez, L., Quesada Carrasco, M., and Díaz-Bonilla, S.: The Beginning of High Mountain Occupations in the Pyrenees. Human Settlements and Mobility from 18,000 cal BC to 2000 cal BC, in: High Mountain Conservation in a Changing World, vol. 62, edited by: Catalan, J., Ninot, J. M., and Aniz, M. M., Springer Nature, Cham, 75–106, https://doi.org/10.1007/978-3-319-55982-7, 2017.

Giesecke, T., Ammann, B., and Brande, A.: Palynological richness and evenness: insights from the taxa accumulation curve, Veget Hist Archaeobot, 23, 217–228, https://doi.org/10.1007/s00334-014-0435-5, 2014.

Giguet-Covex, C., Pansu, J., Arnaud, F., Rey, P.-J., Griggo, C., Gielly, L., Domaizon, I., Coissac, E., David, F., Choler, P., Poulenard, J., and Taberlet, P.: Long livestock farming history and human landscape shaping revealed by lake sediment DNA, Nat Commun, 5, 3211, https://doi.org/10.1038/ncomms4211, 2014.

Giguet-Covex, C., Ficetola, G. F., Walsh, K., Poulenard, J., Bajard, M., Fouinat, L., Sabatier, P., Gielly, L., Messager, E., Develle, A. L., David, F., Taberlet, P., Brisset, E., Guiter, F., Sinet, R., and Arnaud, F.: New insights on lake sediment DNA from the catchment: importance of taphonomic and analytical issues on the record quality, Sci Rep, 9, 14676, https://doi.org/10.1038/s41598-019-50339-1, 2019.

Gil-Romera, G., González-Sampériz, P., Lasheras-Álvarez, L., Sevilla-Callejo, M., Moreno, A., Valero-Garcés, B., López-Merino, L., Carrión, J. S., Pérez Sanz, A., Aranbarri, J., and García-Prieto Fronce, E.: Biomass-modulated fire dynamics during the Last Glacial–Interglacial Transition at the Central Pyrenees (Spain), Palaeogeography, Palaeoclimatology, Palaeoecology, 402, 113–124, https://doi.org/10.1016/j.palaeo.2014.03.015, 2014.

González Bernáldez, F.: Ecología y Paisaje, H. Blume, 1981.

González-Sampériz, P., Valero-Garcés, B., and Carrión, J. S.: Was the Ebro valley a glacial refugium for temperate trees?, Anales de Biología, 8, 2004.

González-Sampériz, P., Valero-Garcés, B. L., Carrión, J. S., Peña-Monné, J. L., García-Ruiz, J. M., and Martí-Bono, C.: Glacial and Lateglacial vegetation in northeastern Spain: New data and a review, Quaternary International, 140–141, 4–20, https://doi.org/10.1016/j.quaint.2005.05.006, 2005.

González-Sampériz, P., Valero-Garcés, B. L., Moreno, A., Jalut, G., García-Ruiz, J. M., Martí-Bono, C., Delgado-Huertas, A., Navas, A., Otto, T., and Dedoubat, J. J.: Climate variability in the Spanish Pyrenees during the last 30,000 yr revealed by the El Portalet sequence, Quat. res., 66, 38–52, https://doi.org/10.1016/j.yqres.2006.02.004, 2006.

González-Sampériz, P., Utrilla, P., Mazo, C., Valero-Garcés, B., Sopena, M., Morellón, M., Sebastián, M., Moreno, A., and Martínez-Bea, M.: Patterns of human occupation during the early Holocene in the Central Ebro Basin (NE Spain) in response to the 8.2 ka climatic event, Quaternary Research, 71, 121–132, https://doi.org/10.1016/j.yqres.2008.10.006, 2009.

González-Sampériz, P., Leroy, S. A. G., Carrión, J. S., Fernández, S., García-Antón, M., Gil-García, M. J., Uzquiano, P., Valero-Garcés, B., and Figueiral, I.: Steppes, savannahs, forests and phytodiversity reservoirs during the Pleistocene in the Iberian Peninsula, Review of Palaeobotany and Palynology, 162, 427–457, https://doi.org/10.1016/j.revpalbo.2010.03.009, 2010.

González-Sampériz, P., Aranbarri, J., Pérez-Sanz, A., Gil-Romera, G., Moreno, A., Leunda, M., Sevilla-Callejo, M., Corella, J. P., Morellón, M., Oliva, B., and Valero-Garcés, B.: Environmental and climate change in the southern Central Pyrenees since the Last Glacial Maximum: A view from the lake records, CATENA, 149, 668–688, https://doi.org/10.1016/j.catena.2016.07.041, 2017.

González-Sampériz, P., Montes, L., Aranbarri, J., Leunda, M., Domingo, R., Laborda, R., Sanjuán, Y., Gil-Romera, G., Lasanta, T., and García-Ruiz, J. M.: Escenarios, tempo e indicadores paleoambientales para la identificación del Antropoceno en el paisaje vegetal del Pirineo Central (NE Iberia), CIG, 45, 167–193, https://doi.org/10.18172/cig.3691, 2019.

Grimm, E. C.: CONISS: a FORTRAN 77 program for stratigraphically constrained cluster analysis by the method of incremental sum of squares, Computers & Geosciences, 13, 13–35, https://doi.org/10.1016/0098-3004(87)90022-7, 1987.

Haile, J., Holdaway, R., Oliver, K., Bunce, M., Gilbert, M. T. P., Nielsen, R., Munch, K., Ho, S. Y. W., Shapiro, B., and Willerslev, E.: Ancient DNA Chronology within Sediment Deposits: Are Paleobiological Reconstructions Possible and Is DNA Leaching a Factor?, Molecular Biology and Evolution, 24, 982–989, https://doi.org/10.1093/molbev/msm016, 2007.

Henne, P. D., Elkin, C., Colombaroli, D., Samartin, S., Bugmann, H., Heiri, O., and Tinner, W.: Impacts of changing climate and land use on vegetation dynamics in a Mediterranean ecosystem: insights from paleoecology and dynamic modeling, Landscape Ecol, 28, 819–833, https://doi.org/10.1007/s10980-012-9782-8, 2013.

Higuera, P. E., Gavin, D. G., Bartlein, P. J., and Hallett, D. J.: Peak detection in sediment - charcoal records: impacts of alternative data analysis methods on fire-history interpretations, Int. J. Wildland Fire, 19, 996, https://doi.org/10.1071/WF09134, 2010.

Hock, R., Rasul, G., Adler, C., Caceres, B., Gruber, S., Hirabayashi, Y., Jackson, M., Kääb, A., Kang, S., Kutuzov, S., Milner, A., Molau, U., Morin, S., Orlove, B., Steltzer, H., Allen, S., Arenson, L., Baneerjee, S., Barr, I., Bórquez, R., Brown, L., Cao, B., Carey, M., Cogley, G., Fischlin, A., A de Sherbinin, Eckert, N., Geertsema, M., Hagenstad, M., Honsberg, M., Hood, E., Huss, M., E Jimenez Zamora, Kotlarski, S., Lefeuvre, P., López-Moreno, J. I., Lundquist, J., Mcdowell, G., Mills, S., Mou, C., Nepal, S., Noetzli, J., Palazzi, E., Pepin, N., Rixen, C., Shahgedanova, M., S McKenzie Skiles, Vincent, C., Viviroli, D., Gesa, A. W., P Yangjee Sherpa, Weyer, N., Wouters, B., Yasunari, T., You, Q., and Zhang, Y.: High Mountain Areas, in: IPCC Special Report on the Ocean and Cryosphere in a Changing Climate, edited by: Pörtner, H. O., Roberts, D. C., Masson-Delmotte, V., Zhai, P., Tignor, M., Poloczanska, E., Mintenbeck, K., Alegría, A., Nicolai, M., Okem, A., Petzold, J., Rama, B., and Weyer, N. M., STATI UNITI D'AMERICA, 2019.

Inácio, L. G., Bernardino, R., Bernardino, S., and Afonso, C.: Acorns: From an Ancient Food to a Modern Sustainable Resource, Sustainability, 16, 9613, https://doi.org/10.3390/su16229613, 2024.

Jalut, G., Esteban Amat, A., Mora, S. R. I., Fontugne, M., Mook, R., Bonnet, L., and Gauquelin, T.: Holocene climatic changes in the western Mediterranean: installation of the Mediterranean climate, Comptes Rendus de l'Académie des Sciences - Series IIA - Earth and Planetary Science, 325, 327–334, https://doi.org/10.1016/S1251-8050(97)81380-8, 1997.

Juggins, S.: CRAN: Package rioja, https://cran.r-project.org/web/packages/rioja/index.html (last access: 29 August 2025), 2024.

Julián-Posada, I., Gil-Romera, G., Garcés-Pastor, S., Heintzman, P. D., Gómez, D., Fillat, F., Moreno, A., Lara-Recuero, J., Bover, P., Montes, L., Sierra, A., Valero-Garcés, B., Alsos, I. G., and González-Sampériz, P.: Neolithic pastoralism and plant community interactions at high altitudes of the Pyrenees, southern Europe, Commun Earth Environ, 6, 48, https://doi.org/10.1038/s43247-025-02023-8, 2025.

Kaltenrieder, P., Procacci, G., Vannière, B., and Tinner, W.: Vegetation and fire history of the Euganean Hills (Colli Euganei) as recorded by Lateglacial and Holocene sedimentary series from Lago della Costa (northeastern Italy), The Holocene, 20, 679–695, https://doi.org/10.1177/0959683609358911, 2010.

Kelly, R. F., Higuera, P. E., Barrett, C. M., and Hu, F. S.: A signal-to-noise index to quantify the potential for peak detection in sediment–charcoal records, Quat. res., 75, 11–17, https://doi.org/10.1016/j.yqres.2010.07.011, 2011.

Knight, C. A., Battles, J. J., Bunting, M. J., Champagne, M., Wanket, J. A., and Wahl, D. B.: Methods for robust estimates of tree biomass from pollen accumulation rates: Quantifying paleoecological reconstruction uncertainty, Front. Ecol. Evol., 10, https://doi.org/10.3389/fevo.2022.956143, 2022.

Kozáková, R., Šamonil, P., Kuneš, P., Novák, J., Kočár, P., and Kočárová, R.: Contrasting local and regional Holocene histories of Abies alba in the Czech Republic in relation to human impact: Evidence from forestry, pollen and anthracological data, The Holocene, 21, 431–444, https://doi.org/10.1177/0959683610385721, 2011.

Laborda, R.: El Neolítico antiguo en el Valle Medio del Ebro. Una visión desde la cerámica y las dataciones radiocarbónicas, Prensas de la Universidad de Zaragoza, 270 pp., 2019.

Laoué, J., Havaux, M., Ksas, B., Tuccio, B., Lecareux, C., Fernandez, C., and Ormeño, E.: Long-term rain exclusion in a Mediterranean forest: response of physiological and physico-chemical traits of Quercus pubescens across seasons, The Plant Journal, 116, 1293–1308, https://doi.org/10.1111/tpj.16424, 2023.

Lepofsky, D. and Lertzman, K.: Documenting ancient plant management in the northwest of North AmericaThis paper was submitted for the Special Issue on Ethnobotany, inspired by the Ethnobotany Symposium organized by Alain Cuerrier,

Montréal Botanical Garden, and held in Montréal at the 2006 annual meeting of the Canadian Botanical Association., Botany, 86, 129–145, https://doi.org/10.1139/B07-094, 2008.

Leunda, M., González-Sampériz, P., Gil-Romera, G., Aranbarri, J., Moreno, A., Oliva-Urcia, B., Sevilla-Callejo, M., and Valero-Garcés, B.: The Late-Glacial and Holocene Marboré Lake sequence (2612 m a.s.l., Central Pyrenees, Spain): Testing high altitude sites sensitivity to millennial scale vegetation and climate variability, Global and Planetary Change, 157, 214–231, https://doi.org/10.1016/j.gloplacha.2017.08.008, 2017.

Leunda, M., González-Sampériz, P., Gil-Romera, G., Bartolomé, M., Belmonte-Ribas, Á., Gómez-García, D., Kaltenrieder, P., Rubiales, J. M., Schwörer, C., Tinner, W., Morales-Molino, C., and Sancho, C.: Ice cave reveals environmental forcing of long-term Pyrenean tree line dynamics, J Ecol, 107, 814–828, https://doi.org/10.1111/1365-2745.13077, 2019.

Leunda, M., Gil-Romera, G., Daniau, A.-L., Benito, B. M., and González-Sampériz, P.: Holocene fire and vegetation dynamics in the Central Pyrenees (Spain), CATENA, 188, 104411, https://doi.org/10.1016/j.catena.2019.104411, 2020.

Leys, B. A., Commerford, J. L., and McLauchlan, K. K.: Reconstructing grassland fire history using sedimentary charcoal: Considering count, size and shape, PLoS ONE, 12, e0176445, https://doi.org/10.1371/journal.pone.0176445, 2017.

López-Merino, L., López-Sáez, J. A., Zapata, M. B. R., and García, M. J. G.: Reconstructing the history of beech (*Fagus sylvatica* L.) in the north-western Iberian Range (Spain): From Late-Glacial refugia to the Holocene anthropic-induced forests, Review of Palaeobotany and Palynology, 152, 58–65, https://doi.org/10.1016/j.revpalbo.2008.04.003, 2008.

Lotter, A., Heiri, O., Brooks, S., Leeuwen, J. N. F., Eicher, U., Schwander, J., and Ammann, B.: Rapid summer temperature changes during Termination 1: multi-proxy reconstructions from Gerzensee (Switzerland)., Quaternary Science Reviews, 103–113, 2012.

Magri, D.: Patterns of post-glacial spread and the extent of glacial refugia of European beech (Fagus sylvatica), Journal of Biogeography, 35, 450–463, https://doi.org/10.1111/j.1365-2699.2007.01803.x, 2008.

Martín-Puertas, C., Valero-Garcés, B. L., Brauer, A., Mata, M. P., Delgado-Huertas, A., and Dulski, P.: The Iberian–Roman Humid Period (2600–1600 cal yr BP) in the Zoñar Lake varve record (Andalucía, southern Spain), Quat. res., 71, 108–120, https://doi.org/10.1016/j.yqres.2008.10.004, 2009.

Matthias, I. and Giesecke, T.: Insights into pollen source area, transport and deposition from modern pollen accumulation rates in lake sediments, Quaternary Science Reviews, 87, 12–23, https://doi.org/10.1016/j.quascirev.2013.12.015, 2014.

Milios, E., Kitikidou, K., and Andreadou, P.: Sprouting characteristics of Quercus pubescens Willd. and Quercus frainetto Ten. trees after a wildfire: To cut or not to cut the burned trees?, Eur J Forest Res, 136, 971–979, https://doi.org/10.1007/s10342-017-1085-9, 2017.

Miras, Y., Ejarque, A., Riera, S., Palet, J. M., Orengo, H., and Euba, I.: Dynamique holocène de la végétation et occupation des Pyrénées andorranes depuis le Néolithique ancien, d'après l'analyse pollinique de la tourbière de Bosc dels Estanyons (2180m, Vall del Madriu, Andorre), Comptes Rendus Palevol, 6, 291–300, https://doi.org/10.1016/j.crpv.2007.02.005, 2007.

Montes, L., Domingo, R., González-Sampériz, P., Sebastián, M., Aranbarri, J., Castaños, P., García-Simón, L. M., Alcolea, M., and Laborda, R.: Landscape, resources and people during the Mesolithic and Neolithic times in NE Iberia: The Arba de Biel Basin, Quaternary International, 403, 133–150, https://doi.org/10.1016/j.quaint.2015.05.041, 2016.

Montes, L., Sebastián, M., Domingo, R., Beguería, S., and García-Ruiz, J. M.: Spatial distribution of megalithic monuments in the subalpine belt of the Pyrenees: Interpretation and implications for understanding early landscape transformation, Journal of Archaeological Science: Reports, 33, 102489, https://doi.org/10.1016/j.jasrep.2020.102489, 2020.

Montserrat, J. M.: Evolución glaciar y postglaciar del clima y la vegetación en la vertiente sur del pirineo : estudio palinológico, Consejo Superior de Investigaciones Científicas (España), 1992.

Moore, P. D., Webb, J. A., and Collinson, M. E.: 1991: Pollen analysis. Oxford: Blackwell Scientific Publications, 1991.

Morales-Molino, C., Steffen, M., Samartin, S., van Leeuwen, J. F. N., Hürlimann, D., Vescovi, E., and Tinner, W.: Long-Term Responses of Mediterranean Mountain Forests to Climate Change, Fire and Human Activities in the Northern Apennines (Italy), Ecosystems, 24, 1361–1377, https://doi.org/10.1007/s10021-020-00587-4, 2021.

Morales-Molino, C., Leunda, M., Morellón, M., Gardoki, J., Ezquerra, F. J., Muñoz Sobrino, C., Rubiales, J. M., and Tinner, W.: Millennial land use explains modern high-elevation vegetation in the submediterranean mountains of Southern Europe, Journal of Biogeography, 49, 1779–1792, https://doi.org/10.1111/jbi.14472, 2022.

Morellón, M., Valero-Garcés, B., Vegas-Vilarrúbia, T., González-Sampériz, P., Romero, Ó., Delgado-Huertas, A., Mata, P., Moreno, A., Rico, M., and Corella, J. P.: Lateglacial and Holocene palaeohydrology in the western Mediterranean region: The Lake Estanya record (NE Spain), Quaternary Science Reviews, 28, 2582–2599, https://doi.org/10.1016/j.quascirev.2009.05.014, 2009.

Morellón, M., Aranbarri, J., Moreno, A., González-Sampériz, P., and Valero-Garcés, B. L.: Early Holocene humidity patterns in the Iberian Peninsula reconstructed from lake, pollen and speleothem records, Quaternary Science Reviews, 181, 1–18, https://doi.org/10.1016/j.quascirev.2017.11.016, 2018.

Moreno, A., López-Merino, L., Leira, M., Marco-Barba, J., González-Sampériz, P., Valero-Garcés, B. L., López-Sáez, J. A., Santos, L., Mata, P., and Ito, E.: Revealing the last 13,500 years of environmental history from the multiproxy record of a mountain lake (Lago Enol, northern Iberian Peninsula), J Paleolimnol, 46, 327–349, https://doi.org/10.1007/s10933-009-9387-7, 2011.

Moreno, A., Svensson, A., Brooks, S. J., Connor, S., Engels, S., Fletcher, W., Genty, D., Heiri, O., Labuhn, I., Perşoiu, A., Peyron, O., Sadori, L., Valero-Garcés, B., Wulf, S., and Zanchetta, G.: A compilation of Western European terrestrial records 60–8 ka BP: towards an understanding of latitudinal climatic gradients, Quaternary Science Reviews, 106, 167–185, https://doi.org/10.1016/j.quascirev.2014.06.030, 2014.

Muñoz Sobrino, C., Ramil-Rego, P., and Gómez-Orellana, L.: Vegetation of the Lago de Sanabria area (NW Iberia) since the end of the Pleistocene: a palaeoecological reconstruction on the basis of two new pollen sequences, Veget Hist Archaeobot, 13, 1–22, https://doi.org/10.1007/s00334-003-0028-1, 2004.

Navarro, L. M. and Pereira, H. M.: Rewilding Abandoned Landscapes in Europe, in: Rewilding European Landscapes, edited by: Pereira, H. M. and Navarro, L. M., Springer International Publishing, Cham, 3–24, https://doi.org/10.1007/978-3-319-12039-3, 2015.

Ninyerola, M., Pons, X., and Roure, J. M.: Atlas Climático Digital de la Península Ibérica. Metodología y Aplicaciones en Bioclimatología y Geobotánica, Universidad Autónoma de Barcelona, Bellaterra Data, 2005.

Oksanen, J., Simpson, G. L., Blanchet, F. G., Kindt, R., Legendre, P., Minchin, P. R., O'Hara, R. B., Solymos, P., Stevens, M. H. H., Szoecs, E., Wagner, H., Barbour, M., Bedward, M., Bolker, B., Borcard, D., Carvalho, G., Chirico, M., Caceres, M. D., Durand, S., Evangelista, H. B. A., FitzJohn, R., Friendly, M., Furneaux, B., Hannigan, G., Hill, M. O., Lahti, L., McGlinn, D.,

Ouellette, M.-H., Cunha, E. R., Smith, T., Stier, A., Braak, C. J. F. T., and Weedon, J.: vegan: Community Ecology Package, https://CRAN.R-project.org/package=vegan, 2022.

Ortu, E., Brewer, S., and Peyron, O.: Pollen-inferred palaeoclimate reconstructions in mountain areas: problems and perspectives, Journal of Quaternary Science, 21, 615–627, https://doi.org/10.1002/jqs.998, 2006.

Oteros-Rozas, E., Ontillera-Sánchez, R., Sanosa, P., Gómez-Baggethun, E., Reyes-García, V., and González, J. A.: Traditional ecological knowledge among transhumant pastoralists in Mediterranean Spain, Ecology and Society, 18, 2013.

Padilla, F. M., Vidal, B., Sánchez, J., and Pugnaire, F. I.: Land-use changes and carbon sequestration through the twentieth century in a Mediterranean mountain ecosystem: Implications for land management, Journal of Environmental Management, 91, 2688–2695, https://doi.org/10.1016/j.jenvman.2010.07.031, 2010.

Parducci, L., Bennett, K. D., Ficetola, G. F., Alsos, I. G., Suyama, Y., Wood, J. R., and Pedersen, M. W.: Ancient plant DNA in lake sediments, New Phytol, 214, 924–942, https://doi.org/10.1111/nph.14470, 2017.

Parducci, L., Nota, K., and Wood, J.: Reconstructing Past Vegetation Communities Using Ancient DNA from Lake Sediments, in: Paleogenomics: Genome-Scale Analysis of Ancient DNA, edited by: Lindqvist, C. and Rajora, O. P., Springer International Publishing, Cham, 163–187, https://doi.org/10.1007/13836_2018_38, 2019.

Pausas, J. G. and Paula, S.: Fuel shapes the fire–climate relationship: evidence from Mediterranean ecosystems, Global Ecology and Biogeography, 21, 1074–1082, https://doi.org/10.1111/j.1466-8238.2012.00769.x, 2012.

Pèlachs, A., Soriano, J. M., and Nadal, J.: Holocene environmental history and human impact in the Pyrenees, Contributions to Science, 421–429, https://doi.org/10.2436/20.7010.01.19, 2007.

Pèlachs, A., Pérez-Obiol, R., Ninyerola, M., and Nadal, J.: Landscape dynamics of Abies and Fagus in the southern Pyrenees during the last 2200 years as a result of anthropogenic impacts, Review of Palaeobotany and Palynology, 156, 337–349, https://doi.org/10.1016/j.revpalbo.2009.04.005, 2009.

Pérez-Díaz, S., López-Sáez, J. A., and Galop, D.: Vegetation dynamics and human activity in the Western Pyrenean Region during the Holocene, Quaternary International, 364, 65–77, https://doi.org/10.1016/j.quaint.2014.10.019, 2015.

Pérez-Obiol, R., Bal, M.-C., Pèlachs, A., Cunill, R., and Soriano, J. M.: Vegetation dynamics and anthropogenically forced changes in the Estanilles peat bog (southern Pyrenees) during the last seven millennia, Veget Hist Archaeobot, 21, 385–396, https://doi.org/10.1007/s00334-012-0351-5, 2012.

Pérez-Sanz, A., González-Sampériz, P., Moreno, A., Valero-Garcés, B., Gil-Romera, G., Rieradevall, M., Tarrats, P., Lasheras-Álvarez, L., Morellón, M., Belmonte, A., Sancho, C., Sevilla-Callejo, M., and Navas, A.: Holocene climate variability, vegetation dynamics and fire regime in the central Pyrenees: the Basa de la Mora sequence (NE Spain), Quaternary Science Reviews, 73, 149–169, https://doi.org/10.1016/j.quascirev.2013.05.010, 2013.

Pla, S. and Catalan, J.: Chrysophyte cysts from lake sediments reveal the submillennial winter/spring climate variability in the northwestern Mediterranean region throughout the Holocene, Clim Dyn, 24, 263–278, https://doi.org/10.1007/s00382-004-0482-1, 2005.

Plieninger, T., Hartel, T., Martín-López, B., Beaufoy, G., Bergmeier, E., Kirby, K., Montero, M. J., Moreno, G., Oteros-Rozas, E., and Van Uytvanck, J.: Wood-pastures of Europe: Geographic coverage, social–ecological values, conservation management, and policy implications, Biological Conservation, 190, 70–79, https://doi.org/10.1016/j.biocon.2015.05.014, 2015.

Power, M. J., Marlon, J., Ortiz, N., Bartlein, P. J., Harrison, S. P., Mayle, F. E., Ballouche, A., Bradshaw, R. H. W., Carcaillet, C., Cordova, C., Mooney, S., Moreno, P. I., Prentice, I. C., Thonicke, K., Tinner, W., Whitlock, C., Zhang, Y., Zhao, Y., Ali, A. A., Anderson, R. S., Beer, R., Behling, H., Briles, C., Brown, K. J., Brunelle, A., Bush, M., Camill, P., Chu, G. Q., Clark, J., Colombaroli, D., Connor, S., Daniau, A.-L., Daniels, M., Dodson, J., Doughty, E., Edwards, M. E., Finsinger, W., Foster, D., Frechette, J., Gaillard, M.-J., Gavin, D. G., Gobet, E., Haberle, S., Hallett, D. J., Higuera, P., Hope, G., Horn, S., Inoue, J., Kaltenrieder, P., Kennedy, L., Kong, Z. C., Larsen, C., Long, C. J., Lynch, J., Lynch, E. A., McGlone, M., Meeks, S., Mensing, S., Meyer, G., Minckley, T., Mohr, J., Nelson, D. M., New, J., Newnham, R., Noti, R., Oswald, W., Pierce, J., Richard, P. J. H., Rowe, C., Sanchez Goñi, M. F., Shuman, B. N., Takahara, H., Toney, J., Turney, C., Urrego-Sanchez, D. H., Umbanhowar, C., Vandergoes, M., Vanniere, B., Vescovi, E., Walsh, M., Wang, X., Williams, N., Wilmshurst, J., and Zhang, J. H.: Changes in fire regimes since the Last Glacial Maximum: an assessment based on a global synthesis and analysis of charcoal data, Clim Dyn, 30, 887–907, https://doi.org/10.1007/s00382-007-0334-x, 2008.

Rasmussen, S. O., Andersen, K. K., Svensson, A. M., Steffensen, J. P., Vinther, B. M., Clausen, H. B., Siggaard-Andersen, M. -L., Johnsen, S. J., Larsen, L. B., Dahl-Jensen, D., Bigler, M., Röthlisberger, R., Fischer, H., Goto-Azuma, K., Hansson, M. E., and Ruth, U.: A new Greenland ice core chronology for the last glacial termination, J. Geophys. Res., 111, 2005JD006079, https://doi.org/10.1029/2005JD006079, 2006.

Rasmussen, S. O., Vinther, B. M., Clausen, H. B., and Andersen, K. K.: Early Holocene climate oscillations recorded in three Greenland ice cores, Quaternary Science Reviews, 26, 1907–1914, https://doi.org/10.1016/j.quascirev.2007.06.015, 2007.

Reille, M.: Pollen et spores d'Europe et d'Afrique du Nord, Laboratoire de Botanique historique et Palynologie, Marseille, 520 pp., 1992.

Reimer, P. J., Austin, W. E. N., Bard, E., Bayliss, A., Blackwell, P. G., Bronk Ramsey, C., Butzin, M., Cheng, H., Edwards, R. L., Friedrich, M., Grootes, P. M., Guilderson, T. P., Hajdas, I., Heaton, T. J., Hogg, A. G., Hughen, K. A., Kromer, B., Manning, S. W., Muscheler, R., Palmer, J. G., Pearson, C., van der Plicht, J., Reimer, R. W., Richards, D. A., Scott, E. M., Southon, J. R., Turney, C. S. M., Wacker, L., Adolphi, F., Büntgen, U., Capano, M., Fahrni, S. M., Fogtmann-Schulz, A., Friedrich, R., Köhler, P., Kudsk, S., Miyake, F., Olsen, J., Reinig, F., Sakamoto, M., Sookdeo, A., and Talamo, S.: The IntCal20 Northern Hemisphere Radiocarbon Age Calibration Curve (0–55 cal kBP), Radiocarbon, 62, 725–757, https://doi.org/10.1017/RDC.2020.41, 2020.

Renssen, H., Seppä, H., Heiri, O., Roche, D. M., Goosse, H., and Fichefet, T.: The spatial and temporal complexity of the Holocene thermal maximum, Nature Geosci, 2, 411–414, https://doi.org/10.1038/ngeo513, 2009.

Revelles, J.: Archaeoecology of Neolithisation. Human-environment interactions in the NE Iberian Peninsula during the Early Neolithic, Journal of Archaeological Science: Reports, 15, 437–445, https://doi.org/10.1016/j.jasrep.2016.02.004, 2017.

Rey, F., Gobet, E., Schwörer, C., Wey, O., Hafner, A., and Tinner, W.: Causes and mechanisms of synchronous succession trajectories in primeval Central European mixed *Fagus sylvatica* forests, Journal of Ecology, 107, 1392–1408, https://doi.org/10.1111/1365-2745.13121, 2019.

Rijal, D. P., Heintzman, P. D., Lammers, Y., Yoccoz, N. G., Lorberau, K. E., Pitelkova, I., Goslar, T., Ancin-Murguzur, F. J., Salonen, J. S., Helmens, KarinF., Bakke, J., Edwards, M. E., Alm, T., Bråthen, K., and Alsos, I. G.: Sedimentary ancient DNA shows terrestrial plant richness continuously increased over the Holocene in northern Fennoscandia, SCIENCE ADVANCES, 17, 2021.

Rius, D., Vannière, B., and Galop, D.: Fire frequency and landscape management in the northwestern Pyrenean piedmont, France, since the early Neolithic (8000 cal. BP), The Holocene, 19, 847–859, https://doi.org/10.1177/0959683609105299, 2009.

Rius, D., Vannière, B., Galop, D., and Richard, H.: Holocene fire regime changes from multiple-site sedimentary charcoal analyses in the Lourdes basin (Pyrenees, France), Quaternary Science Reviews, 30, 1696–1709, https://doi.org/10.1016/j.quascirev.2011.03.014, 2011.

Rius, D., Vanniére, B., and Galop, D.: Holocene history of fire, vegetation and land use from the central Pyrenees (France), Quat. res., 77, 54–64, https://doi.org/10.1016/j.yqres.2011.09.009, 2012.

Roberts, N., Stevenson, T., Davis, B., Cheddadi, R., Brewster, S., and Rosen, A.: Holocene climate, environment and cultural change in the circum-Mediterranean region, in: Past Climate Variability through Europe and Africa, edited by: Battarbee, R. W., Gasse, F., and Stickley, C. E., Springer Netherlands, Dordrecht, 343–362, https://doi.org/10.1007/978-1-4020-2121-3_17, 2004.

Ruiz-Alonso, M., Pérez-Díaz, S., and López-Sáez, J. A.: From glacial refugia to the current landscape configuration: permanence, expansion and forest management of Fagus sylvatica L. in the Western Pyrenean Region (Northern Iberian Peninsula), Veget Hist Archaeobot, 28, 481–496, https://doi.org/10.1007/s00334-018-0707-6, 2019.

Sánchez-Morales, M., Pèlachs, A., García-Codron, J. C., Carracedo, V., and Pérez-Obiol, R.: Landscape dynamics and fire regime since 17,550 cal yr BP in the Cantabrian region (La Molina peat bog, Puente Viesgo, Spain), Quaternary Science Reviews, 278, 107373, https://doi.org/10.1016/j.quascirev.2022.107373, 2022.

Schnurrenberger, D., Russell, J., and Kelts, K.: Classification of lacustrine sediments based on sedimentary components, Journal of Paleolimnology, 29, 141–154, https://doi.org/10.1023/A:1023270324800, 2003.

Schwörer, C., Colombaroli, D., Kaltenrieder, P., Rey, F., and Tinner, W.: Early human impact (5000–3000 BC) affects mountain forest dynamics in the Alps, Journal of Ecology, 103, 281–295, https://doi.org/10.1111/1365-2745.12354, 2015.

Seppä, H., Alenius, T., Muukkonen, P., Giesecke, T., Miller, P. A., and Ojala, A. E. K.: Calibrated pollen accumulation rates as a basis for quantitative tree biomass reconstructions, The Holocene, 19, 209–220, https://doi.org/10.1177/0959683608100565, 2009.

Sierra, A., Bréhard, S., Montes, L., Utrilla, P., and Saña, M.: Sheep exploitation and husbandry in first farming societies: from production to consumption in Central Pyrenees in the Early Neolithic, Archaeol Anthropol Sci, 11, 5813–5829, https://doi.org/10.1007/s12520-019-00907-3, 2019.

Steinbauer, M. J., Grytnes, J.-A., Jurasinski, G., Kulonen, A., Lenoir, J., Pauli, H., Rixen, C., Winkler, M., Bardy-Durchhalter, M., Barni, E., Bjorkman, A. D., Breiner, F. T., Burg, S., Czortek, P., Dawes, M. A., Delimat, A., Dullinger, S., Erschbamer, B., Felde, V. A., Fernández-Arberas, O., Fossheim, K. F., Gómez-García, D., Georges, D., Grindrud, E. T., Haider, S., Haugum, S. V., Henriksen, H., Herreros, M. J., Jaroszewicz, B., Jaroszynska, F., Kanka, R., Kapfer, J., Klanderud, K., Kühn, I., Lamprecht, A., Matteodo, M., di Cella, U. M., Normand, S., Odland, A., Olsen, S. L., Palacio, S., Petey, M., Piscová, V., Sedlakova, B., Steinbauer, K., Stöckli, V., Svenning, J.-C., Teppa, G., Theurillat, J.-P., Vittoz, P., Woodin, S. J., Zimmermann, N. E., and Wipf, S.: Accelerated increase in plant species richness on mountain summits is linked to warming, Nature, 556, 231–234, https://doi.org/10.1038/s41586-018-0005-6, 2018.

Stockmarr, J. A.: Tablets with spores used in absolute pollen analysis, Pollen spores, 13, 615–621, 1971.

Tarrats, P., Heiri, O., Valero-Garcés, B., Cañedo-Argüelles, M., Prat, N., Rieradevall, M., and González-Sampériz, P.: Chironomid-inferred Holocene temperature reconstruction in Basa de la Mora Lake (Central Pyrenees), The Holocene, 28, 1685–1696, https://doi.org/10.1177/0959683618788662, 2018.

Terhürne-Berson, R., Litt, T., and Cheddadi, R.: The spread of Abies throughout Europe since the last glacial period: combined macrofossil and pollen data, Veget Hist Archaeobot, 13, 257–268, https://doi.org/10.1007/s00334-004-0049-4, 2004.

Tinner, W. and Hu, F. S.: Size parameters, size-class distribution and area-number relationship of microscopic charcoal: relevance for fire reconstruction, The Holocene, 13, 499–505, https://doi.org/10.1191/0959683603hl615rp, 2003.

Tinner, W. and Lotter, A.: Holocene expansions of *Fagus sylvatica* and *Abies alba* in Central Europe: where are we after eight decades of debate?, Quaternary Science Reviews, 25, 526–549, https://doi.org/10.1016/j.quascirev.2005.03.017, 2006.

Tinner, W., Conedera, M., Gobet, E., Hubschmid, P., Wehrli, M., and Ammann, B.: A palaeoecological attempt to classify fire sensitivity of trees in the southern Alps, The Holocene, 10, 565–574, https://doi.org/10.1191/095968300674242447, 2000.

Tinner, W., Colombaroli, D., Heiri, O., Henne, P. D., Steinacher, M., Untenecker, J., Vescovi, E., Allen, J. R. M., Carraro, G., Conedera, M., Joos, F., Lotter, A. F., Luterbacher, J., Samartin, S., and Valsecchi, V.: The past ecology of *Abies alba* provides new perspectives on future responses of silver fir forests to global warming, Ecological Monographs, 83, 419–439, https://doi.org/10.1890/12-2231.1, 2013.

Trotta, G., Cadez, L., Boscutti, F., Vuerich, M., Asquini, E., Boscarol, G., Cingano, P., Azzani, G., Pischedda, S., Tomao, A., and Alberti, G.: Interpreting the shifts in forest structure, plant community composition, diversity, and functional identity by using remote sensing-derived wildfire severity, Fire Ecology, 20, 94, https://doi.org/10.1186/s42408-024-00330-7, 2024.

Utrilla, P., Domingo, R., Montes, L., Mazo, C., Rodanés, J. M., Blasco, F., and Alday, A.: The Ebro Basin in NE Spain: A crossroads during the Magdalenian, Quaternary International, 272–273, 88–104, https://doi.org/10.1016/j.quaint.2012.04.024, 2012.

Valero-Garcés, B. L., González-Sampériz, P., Delgado-Huertas, A., Navas, A., Machín, J., and Kelts, K.: Lateglacial and Late Holocene environmental and vegetational change in Salada Mediana, central Ebro Basin, Spain, Quaternary International, 73–74, 29–46, https://doi.org/10.1016/S1040-6182(00)00063-X, 2000.

Van Der Horst, A., Tinner, W., Ezquerra, F. J., Gobet, E., Lotter, A. F., Morellón, M., Muñoz Sobrino, C., Niffenegger, C., Schwörer, C., Szidat, S., and Morales-Molino, C.: Late-glacial and Holocene shifts in the mountain landscapes of the Cantabrian range (northern Spain) in response to changing climate, fire occurrence and land use, Quaternary Science Reviews, 342, 108899, https://doi.org/10.1016/j.quascirev.2024.108899, 2024.

Vannière, B., Power, M. J., Roberts, N., Tinner, W., Carrión, J., Magny, M., Bartlein, P., Colombaroli, D., Daniau, A. L., Finsinger, W., Gil-Romera, G., Kaltenrieder, P., Pini, R., Sadori, L., Turner, R., Valsecchi, V., and Vescovi, E.: Circum-Mediterranean fire activity and climate changes during the mid-Holocene environmental transition (8500-2500 cal. BP), The Holocene, 21, 53–73, https://doi.org/10.1177/0959683610384164, 2011.

Vannière, B., Blarquez, O., Rius, D., Doyen, E., Brücher, T., Colombaroli, D., Connor, S., Feurdean, A., Hickler, T., Kaltenrieder, P., Lemmen, C., Leys, B., Massa, C., and Olofsson, J.: 7000-year human legacy of elevation-dependent European fire regimes, Quaternary Science Reviews, 132, 206–212, https://doi.org/10.1016/j.quascirev.2015.11.012, 2016.

Vidaller, I., Moreno, A., González-Sampériz, P., Pla-Rabés, S., Medialdea, A., Del Val, M., López-Moreno, J. I., and Valero-Garcés, B.: The last deglaciation in the central Pyrenees: The 47 ka Pllan d'Están paleolake record (Ésera valley), CATENA, 241, 108059, https://doi.org/10.1016/j.catena.2024.108059, 2024.

Villar, L. and Sesé, A.: Aspectos sobre la Flora y vegetación de la alta Cuenca del gállego, 1999.

Vincze, I., Orbán, I., Birks, H. H., Pál, I., Finsinger, W., Hubay, K., Marinova, E., Jakab, G., Braun, M., Biró, T., Tóth, M., Dănău, C., Ferencz, I. V., and Magyari, E. K.: Holocene treeline and timberline changes in the South Carpathians (Romania): Climatic and anthropogenic drivers on the southern slopes of the Retezat Mountains, The Holocene, 27, 1613–1630, https://doi.org/10.1177/0959683617702227, 2017.

Viviroli, D., Archer, D. R., Buytaert, W., Fowler, H. J., Greenwood, G. B., Hamlet, A. F., Huang, Y., Koboltschnig, G., Litaor, M. I., López-Moreno, J. I., Lorentz, S., Schädler, B., Schreier, H., Schwaiger, K., Vuille, M., and Woods, R.: Climate change and mountain water resources: overview and recommendations for research, management and policy, Hydrol. Earth Syst. Sci., 15, 471–504, https://doi.org/10.5194/hess-15-471-2011, 2011.

van Vugt, L., Garcés-Pastor, S., Gobet, E., Brechbühl, S., Knetge, A., Lammers, Y., Stengele, K., Alsos, I. G., Tinner, W., and Schwörer, C.: Pollen, macrofossils and *sed*aDNA reveal climate and land use impacts on Holocene mountain vegetation of the Lepontine Alps, Italy, Quaternary Science Reviews, 296, 107749, https://doi.org/10.1016/j.quascirev.2022.107749, 2022.

Walker, M., Head, M. J., Berkelhammer, M., Björck, S., Cheng, H., Cwynar, L., Fisher, D., Gkinis, V., Long, A., Lowe, J., Newnham, R., Rasmussen, S. O., and Weiss, H.: Formal ratification of the subdivision of the Holocene Series/Epoch (Quaternary System/Period): two new Global Boundary Stratotype Sections and Points (GSSPs) and three new stages/subseries, Episodes, 41, 213–223, https://doi.org/10.18814/epiiugs/2018/018016, 2018.

Wick, L. and Möhl, A.: The mid-Holocene extinction of silver fir (Abies alba) in the Southern Alps: a consequence of forest fires? Palaeobotanical records and forest simulations, Veget Hist Archaeobot, 15, 435–444, https://doi.org/10.1007/s00334-006-0051-0, 2006.

Wick, L., Van Leeuwen, J. F. N., Van Der Knaap, W. O., and Lotter, A. F.: Holocene vegetation development in the catchment of Sägistalsee (1935 m asl), a small lake in the Swiss Alps, Journal of Paleolimnology, 30, 261–272, 2003.

Wickham, H., Chang, W., Henry, L., Pedersen, T. L., Takahashi, K., Wilke, C., Woo, K., Yutani, H., Dunnington, D., Brand, T. van den, Posit, and PBC: ggplot2: Create Elegant Data Visualisations Using the Grammar of Graphics (3.5.2), https://cran.r-project.org/web/packages/ggplot2/index.html (last access: 29 August 2025), 2025.

Yoccoz, N. G., Bråthen, K. A., Gielly, L., Haile, J., Edwards, M. E., Goslar, T., Von STEDINGK, H., Brysting, A. K., Coissac, E., Pompanon, F., Sønstebø, J. H., Miquel, C., Valentini, A., De BELLO, F., Chave, J., Thuiller, W., Wincker, P., Cruaud, C., Gavory, F., Rasmussen, M., Gilbert, M. T. P., Orlando, L., Brochmann, C., Willerslev, E., and Taberlet, P.: DNA from soil mirrors plant taxonomic and growth form diversity, Molecular Ecology, 21, 3647–3655, https://doi.org/10.1111/j.1365-294X.2012.05545.x, 2012.